International Energy Agency
Photovoltaic Power Systems Programme

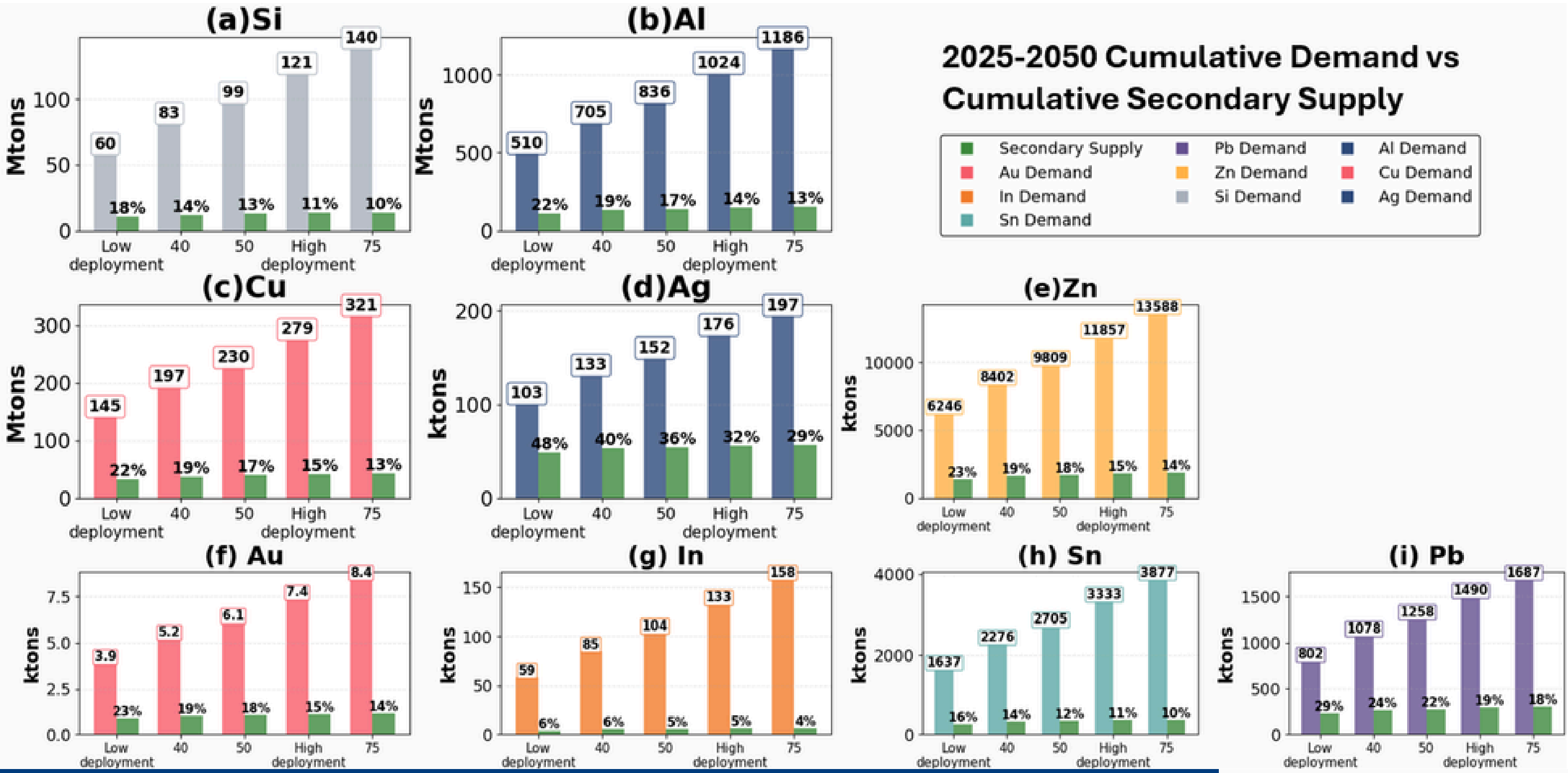

Task 12 PV Sustainability

PVPS

Primary and Secondary Material Flows for the Future Global Deployment of Silicon-based Photovoltaic Systems

2026

Report IEA-PVPS T12-34:2026

What is IEA PVPS TCP?

The International Energy Agency (IEA), founded in 1974, is an autonomous body within the framework of the Organization for Economic Cooperation and Development (OECD). The Technology Collaboration Programme (TCP) was created with a belief that the future of energy security and sustainability starts with global collaboration. The programme is made up of 6 000 experts across government, academia, and industry dedicated to advancing common research and the application of specific energy technologies.

The IEA Photovoltaic Power Systems Programme (IEA PVPS) is one of the TCP's within the IEA and was established in 1993. The mission of the programme is to "enhance the international collaborative efforts which facilitate the role of photovoltaic solar energy as a cornerstone in the transition to sustainable energy systems." In order to achieve this, the Programme's participants have undertaken a variety of joint research projects in PV power systems applications. The overall programme is headed by an Executive Committee, comprised of one delegate from each country or organisation member, which designates distinct 'Tasks,' that may be research projects or activity areas.

The 28 IEA PVPS participating countries are Australia, Austria, Belgium, Canada, China, Denmark, Finland, France, Germany, India, Israel, Italy, Japan, Korea, Lithuania, Malaysia, Morocco, the Netherlands, Norway, Portugal, South Africa, Spain, Sweden, Switzerland, Thailand, Turkiye, the United Kingdom and the United States of America. The European Commission, Solar Power Europe and the Solar Energy Research Institute of Singapore are also members.

Visit us at: www.iea-pvps.org

What is IEA PVPS Task 12?

The goal of Task 12 is to foster international cooperation and knowledge sharing on the sustainable aspects of PV technology, emphasizing environmental and social factors. Its mission is to provide essential information to stakeholders, enhancing consumer and policy-maker confidence in PV systems, and thereby accelerating the shift towards sustainable energy. The objectives of Task 12 are to: (1) Quantify PV electricity's environmental profile to enhance supply chain sustainability and enable comparisons with other energy technologies. (2) Enhance PV technology and materials circularity through novel analysis, legislative tracking, and technical standards development. (3) Investigate synergies between PV system deployment and its environmental and ecosystem impacts. (4) Identify and tackle both real and perceived social and socio-economic challenges to PV market growth. (5) Share analytical findings with technical experts, policymakers, and the public.

Task 12 is operated jointly by the National Laboratory of the Rockies (NLR) and TotalEnergies. Support from the U.S. Department of Energy and TotalEnergies is gratefully acknowledged.

SUGGESTED CITATION

Abdelbaky, M., Xu, C., Isabella, O., Vogt, M.R. (2026). Heath, G. (Ed.), *Primary and Secondary Material Flows for the Future Global Deployment of Silicon-based Photovoltaic Systems* (Report No. T12-34:2026). IEA PVPS Task 12. DOI: 10.69766/WQPE7074

INTERNATIONAL ENERGY AGENCY

PHOTOVOLTAIC POWER SYSTEMS PROGRAMME

Primary and Secondary Material Flows for the Future Global Deployment of Silicon-based Photovoltaic Systems

IEA PVPS
Task 12
PV Sustainability

Report IEA-PVPS T12-34:2026
September 2026

ISBN: 978-1-923734-13-5
DOI: 10.69766/WQPE7074

AUTHORS

Main Authors

Mohammad Abdelbaky, Delft University of Technology, The Netherlands
Chengjian Xu, Delft University of Technology, The Netherlands
Olindo Isabella, Delft University of Technology, The Netherlands
Malte R. Vogt, Delft University of Technology, The Netherlands

Editor

Garvin Heath, National Lab of the Rockies, USA

Task Managers

Garvin Heath, National Lab of the Rockies, USA
Etienne Drahi, TotalEnergies, France

TABLE OF CONTENTS

LIST OF FIGURES

LIST OF TABLES

ACKNOWLEDGEMENTS

We sincerely thank Mário Aliang and Penghui Xie for their master’s thesis work, which provided valuable input to this report, and Nithin Vakeri Perunthottathil for their careful review and constructive feedback that helped refine the results. This report also benefited from valuable feedback from IEA-PVPS Task 12 members, which further strengthened the content of this report. We also thank financial support from the BURST project, that has received funding from the European Union's Horizon Europe Programme under GA No. 101146684.

LIST OF ABBREVIATIONS

ADP_{UR}	Abiotic Depletion Potential, ultimate reserves
ADP_{ER}	Abiotic Depletion Potential, economic reserves
Al	Aluminum
Al-BSF	Aluminum back surface field
BiLSTM	Bidirectional Long Short-Term Memory
BOS	Balance-of-system
CAGR	Compound annual growth rate
Cu	Copper
c-Si	Crystalline silicon
dMFA	Dynamic material flow analysis
EoL	End-of-life
EJ	Exajoules
Gtons	Gigatons
GWp	Gigawatt-peak
Au	Gold
In	Indium
ITO	Indium tin oxide
ESSENZ	Integrated Method to Assess Resource-Use Efficiency method
IBC	Interdigitated back contact
IEA	International Energy Agency
IRENA	International Renewable Energy Agency
ITRPV	International Technology Roadmap for Photovoltaics
ktons	kilotons
kWp	Kilowatt-peak
LUT	Lappeenranta-Lahti University of Technology
Pb	Lead
Mtons Sb eq.	Megatons antimony equivalents
Mtons	Million metric tons
mg	milligrams
NZE	Net Zero Emissions by 2050 Scenario
OAT	One-at-a-time

PERC	Passivated emitter and rear contact
Pvk-Si-tandem	Perovskite-silicon tandem
Si	Silicon
SHJ	Silicon heterojunction cells
Ag	Silver
PV	Solar photovoltaic
SOP_{URR}	Surplus Ore Potential, Ultimate Recoverable Resources
TWp	Terawatt-peak
Sn	Tin
TCO	Transparent conductive oxide
TOPCon	Tunnel oxide passivated contact
Wp	Watt-peak
w%	weight percent
Zn	Zinc

EXECUTIVE SUMMARY

The anticipated expansion in PV installed capacity will increase demand for raw materials necessary for manufacturing and deployment. This aligns with global decarbonization scenarios and recent research which identify rapid expansion of renewable energy capacity as “the single largest driver” of near-term emissions reductions on pathways to net-zero by 2050 [1]. Silicon-based PV dominates global production (~98%), consequently this report focuses on Silicon based PV [2], [3], [4]. Nevertheless, a number of silicon-based PV materials are classified as “critical” in several major economies based on region-specific assessments of potential supply disruptions and economic importance [5]. Recent estimates suggest that annual PV demand could peak at approximately 40% of global silicon production, 44% of silver, 25% of copper [6], which poses potential constraints to large-scale PV deployment. Despite growing attention to this topic in the literature, there are two clear gaps in understanding: (1) evaluating raw material demand at the system level with respect to ongoing technological shifts, and (2) accounting for dynamic reductions in material intensity that are already reshaping the scale of future demand.

This report presents a dynamic material flow analysis (dMFA) model for estimating future silicon-based PV system-related raw material demand, secondary supply, and in-use stock, with deployment scenarios ranging from 29 TWp to 75 TWp of installed global silicon-based PV capacity by 2050. In this report, ‘secondary supply’ refers to the material content of modeled EoL PV outflows under the assumed collection and recovery conditions. Unless otherwise specified, these estimates represent theoretical availability in the waste stream and do not imply that the material can be fully recovered, purified to PV-grade specifications, or reintegrated into PV manufacturing. The model assumes that future PV deployment will continue to be dominated by silicon-PV. Within that, it accounts for expected shifts in the future market share of including aluminum back surface field (Al-BSF), mainly for sales prior to 2025, as well as passivated emitter and rear contact (PERC), tunnel oxide passivated contact (TOPCon), silicon heterojunction (SHJ), interdigitated back contact (IBC), and perovskite-silicon-based tandem (Pvk-Si-tandem) technologies. Moreover, the model accounts for reductions in material intensity as manufacturing processes become more efficient, performance parameters improve, and materials are substituted or phased out. The analysis focuses on nine key elements: aluminum, copper, indium, lead, silicon, silver, gold, tin, and zinc. Results for other PV materials are aggregated at the component level.

The cell level is modeled based on the silicon wafer and the additional functional layers common to commercial cells, while the module level includes front and back glass, copper cell interconnections, as well as an aluminum frame. At the system level, a simplified bill of materials is applied for balance-of-system components to represent average material requirements per installed capacity, without distinguishing between different inverter configurations or cable layouts. System components excluded from the analysis, including foundations, floating structures, control systems, and battery storage, are discussed further in the limitations section. This study assumed full collection and 100% recycling efficiency for the future waste stream generated to provide a theoretical upper-bound estimate of total recycled material mass from retired PV systems. A sensitivity analysis is performed to determine the impact of uncertain future deployment scale and other technological factors on the silicon-based PV sector demand for key materials. Finally, the projected material demands of the global silicon-based PV sector are then evaluated in terms of resource depletion using the Abiotic Depletion Potential, ultimate reserves (ADP_{UR}) method, economic scarcity using the Abiotic Depletion Potential, economic reserves (ADP_{ER}) method, resource quality with the

Surplus Ore Potential, Ultimate Recoverable Resources (SOP_{URR}) method, and resource criticality with the Integrated Method to Assess Resource-Use Efficiency (ESSENZ) method.

According to the dMFA model results, the global silicon-based PV sector is projected to consume between 145 and 280 million metric tons of copper cumulatively between 2025 to 2050, depending on the scale of future deployment. This demand is primarily driven by cables (75w%) and inverter (13w%) components. For aluminum, the cumulative demand from 2025 to 2050 is projected to range from 510 to 1 100 million metric tons. Mounting structures account for around 70w% of demand on average, with their share increasing from 66w% in 2025 to 72w% by 2050. The share of aluminum demand due to module frames is expected to decline from 29% to 23% between 2025 and 2050 due to the gradual adoption of frameless module designs. For silicon, cumulative 2025-2050 demand is projected to range from 60 to 120 million metric tons of solar-grade silicon, with more than 20% of the input silicon lost during wafer slicing. For silver, the cumulative 2025-2050 demand is expected to range between 100 000 and 200 000 metric tons, strongly dependent on the future market share of copper metallization and silver paste loading. The cumulative 2025-2050 indium demand is expected to range between 60 000 and 160 000 metric tons, strongly dependent on the future market share of ITO-based technologies. Tin demand comes primarily from solder alloys, with a minor contribution from ITO layers, and may range from 1-3 million metric tons.

The results show that copper is the PV material with potentially the biggest bottleneck in primary supply for future sector demand. Copper demand by the PV sector will peak in the mid-2040s at 7-15 million tons per year, equivalent to 30w%-65w% of the current annual global mine production [7]. Previous studies show that not all countries prioritize mine capacity expansion, and despite copper mining capacity growing at a 3% CAGR, a supply gap of 10.5-11.5 million metric tons is projected by 2035 [8], [9]. Peak annual demand for solar-grade silicon may range between 3 and 6 million metric tons by 2040, against current global capacity of about 3 million metric tons [10]. However, continued overcapacity in China and capacity additions from project pipelines suggest that supply constraints may be less severe [11], [12]. For silver, 2025-2050 cumulative demand represents roughly 15w%-30w% of current global reserve estimate [7], while annual use in PV cells is expected to peak at 9 000 metric tons, even in high-deployment scenarios. This is only a slight increase over the 8 600 metric tons estimated for 2024 shipments [13]. Tin cumulative demand between 2025 and 2050 could amount to 30w%-64w% of the estimated global Sn reserves reported for 2024 [7], depending on the deployment scenario. For all deployment scenarios, cumulative 2025-2050 indium demand is projected to surpass the most recent global reserve and resource estimate of 50 000 metric tons (2009 data [14], due to lack of a more recent authoritative estimate) by the mid-2040s. Nonetheless, reserve estimates and mine production figures evolve over time, and comparisons with future demand should be interpreted accordingly. Based on the latest figures replacement of indium in transparent conductive oxides (TCOs) is necessary for PV deployment at terawatt per year scale. Furthermore, alternative TCO materials are being tested, but they remain at a low technology readiness level due to varying stability, performance, and cost profiles [15], [16], which may limit their market penetration and contribution to reductions to future indium demand. Continued development of replacement material(s) for indium in TCOs, or reduction in quantity used per module, will be important for the indium consuming parts of the PV industry.

From 2025 to 2050, the mass of materials considered herein from decommissioned PV systems is expected to equal 15-20% of the total demand for those same materials over that period. This limited potential for closed-loop recycling is partly attributed to long product lifetime, which delays the availability of recyclable material, in addition to the purity of recovered materials [17]. However, exceptions for this trend are indium and silver. For indium, the relatively late commercialization and the expected large future market share of ITO-based technologies indicate that more than 90% of cumulative demand will remain in in-use stock by 2050, with the waste stream contributing only the remainder. Total silver mass in future silicon-based PV waste may supply 30-45w% of the cumulative demand between 2025 and 2050.

Based on the projected cumulative raw material demands during the timeframe of this study, the ADP_{UR} method identifies gold used in inverters as the largest contributor to resource depletion impacts (56%), followed by copper (33%) used mostly in cables, and silver (9%) used in cells. Hypothetically, 100% closed-loop recycling could reduce ADP_{UR} impacts by 25% and 17% under low and high deployment scenarios, respectively. The ESSENZ method identifies indium as the main driver of criticality impacts (75%) due to limited reserves and concentration of global refining capacity, followed by tin (9%) and silver (6%). Hypothetical 100% closed-loop recycling may potentially reduce overall criticality impacts by 10% at most, while increasing the relative contribution of indium to the ESSENZ score to 79% as its total mass in future silicon-based PV waste does not match the rapidly growing demand.

The material constraints identified in this study are presented at a time of rapid market expansion. Global PV module prices reached historic lows in 2024-2025 [18], which accelerated deployment beyond earlier International Energy Agency and BloombergNEF forecasts [19]. Meanwhile, the EU Critical Raw Materials Act [20], the US Inflation Reduction Act [21], and India's Production Linked Incentive scheme for solar manufacturing [22], together with ongoing trade tensions, are shaping manufacturing investment decisions and influencing where PV manufacturing capacity will be built over the coming decade [23]. Nevertheless, the findings of this study indicate that material efficiency improvements and material substitution strategies should be considered alongside incentives for domestic production and processing when designing policies to support PV deployment.

1 INTRODUCTION

Outlooks from energy transition scenarios present promising trajectories for increased deployment of photovoltaic (PV) systems. Global installed PV capacity for electricity generation may exceed 20 terawatt-peak (TWp) by 2050, as outlined in the Net Zero Emissions by 2050 (NZE) from the International Energy Agency (IEA) and the 1.5 °C pathway from the International Renewable Energy Agency (IRENA) [24], [25]. The IEA NZE scenario further projects approximately 145 exajoules (EJ) of PV-generated energy allocated to for electricity services and electrified heat supply (e.g., heat pumps) by 2050, with an additional 123 EJ used for the production of low-emission hydrogen-based fuels. Higher 2050 deployment projections have been reported in the literature; for example, Bogdanov et al. estimate 63 TWp of installed capacity, assuming electrification of 89% of total primary energy demand (including for heating and water desalination) [26], while Haegel et al. envision up to 75 TWp installed capacity [27]. The scale of PV deployment projected under these scenarios entails significant raw material requirements, which differ considerably from those of other renewable energy technologies. For example, while PV and wind share common bulk materials such as steel, concrete, aluminum, copper, and glass, their intensities differ: wind turbines require significantly more concrete and steel per MW, whereas PV systems are more intensive in glass and aluminum [28]. Beyond bulk materials, PV relies on a distinct set of specialty materials including silicon metal, indium, gallium, tellurium, and selenium

Recent studies have assessed the resource-use impacts of scaling PV installed capacity, each with distinct strengths and limitations. Frischknecht & Krebs (2022) evaluated resource-use impacts associated with the generation of 1 kilowatt hour electricity from a residential rooftop PV installation using four impact category indicators: (1) resource depletion using the Abiotic Depletion Potential, ultimate reserves (ADP_{UR}) method, (2) economic scarcity using the Abiotic Depletion Potential, economic reserves (ADP_{ER}) method, (3) resource quality with the Surplus Ore Potential, Ultimate Recoverable Resources (SOP_{URR}) method, and (4) resource criticality with the Integrated Method to Assess Resource-Use Efficiency (ESSENZ) [29]. The study identified gold (Au), silver (Ag), and copper (Cu) as the main drivers of resource-use impacts. However, the analysis was limited to impacts expressed per kilowatt hour, and thus did not capture the total raw material demands of large-scale deployment. Furthermore, it aggregates all mono-crystalline silicon (c-Si)-based PV technologies into a single bill of materials, neglecting the substantial variation in material composition across different cell technologies.

By modeling material consumption in PV technologies and defining upper limits for material use at certain fraction of global annual supply, Zhang et al. identified Ag, bismuth (Bi), and indium (In) as the main bottlenecks to large-scale deployment of c-Si PV technologies [30]. They estimated sustainable annual manufacturing capacities of 77 Gigawatt-peak (GWp) for silver-limited passivated emitter and rear contact (PERC), 227 GWp for silver-limited tunnel oxide passivated contact (TOPCon), and 37 GWp for indium-limited silicon heterojunction (SHJ). The authors also derived corresponding material-intensity targets of 2 milligrams (mg)/Wp for silver, 0.38 mg/Wp for indium, and 1.8 mg/Wp for bismuth. In a follow-up study, the authors investigated perovskite solar cells and identified indium and iodine as the main bottlenecks [31]. They also concluded that under the assumption that only 20% of the global primary material supply is used and that the perovskite cells are indium-free with iodine usage well controlled, sustainable manufacturing capacity would be capped at 1 TWp/year. Several of the assumptions made in these studies, however, are no longer representative of current industrial progress, such as cell efficiency and wafer thickness.

Existing literature on future raw material demand of the global PV sector is extensive, focusing particularly on technological progress at the cell and module level. Using technology-dependent learning curves, Hallam et al. estimated that cumulative silver demand by 2050 could exceed 450 kilotons (ktons) [32]. However, this study assumed a lower end of silver intensity at 5 mg/Wp, and did not consider copper metallization with little to no silver content. This was due to the low readiness level of these technologies at the time of the study, but recent solar cells demonstrations have reduced silver material intensity to 2 mg/W [33], [34]. Other studies projected that while silicon material intensity would decrease from 3 000 tons/GWp in 2021 to 1-1.5 ktons/GWp by 2050, but net annual demand would likely increase due to increased production capacity [35], [36]. A recent study by the European Commission assessed future PV raw material demand in the EU and globally using a system□level material flow analysis, with a particular focus on critical raw materials [6]. The study projects a three-fold increase in annual demand for silver, copper, aluminum, and solar glass between 2022 and 2030, followed by marginal changes from 2030 to 2050 due to efficiency gains. Indium is an exception to this trend, with annual demand expected to increase 8 times by 2030 due to the increased market share of indium-containing technologies. As such, PV demand could peak at approximately 40% of global silicon production, 44% of silver, 25% of copper. However, the study takes little account of the nuances in demand for non-critical (or not-yet-critical) raw materials as a result of technological changes, and estimates the secondary supply of PV raw materials based on a fixed lifetime assumption for the put-on-market product stream.

A compelling literature study is the highly-parameterized model developed by Xu et al. to characterize the annual inflow of various c-Si-based PV module technologies on the market and the resulting raw material demands [37]. Model results indicate steep increases in critical raw material demand, with indium demand in 2050 projected to increase by up to >200-fold and up to >20-fold for silver relative to 2022 levels, and strongly dependent on the future market share of PV technologies. The highest material intensities are associated with SHJ and perovskite-silicon-based tandem (Pvk-Si-tandem) technologies. The 2050 demand for silicon (Si), aluminum (Al), copper (Cu), and tin (Sn) were projected to increase 2-20 times relative to 2022 levels, depending on technology development parameters such as wafer thickness and module efficiency. While this model provides valuable insights, it is based on data from 2022 and would benefit from integrating the latest trends outlined in the International Technology Roadmap for Photovoltaics (ITRPV) 2025 report, particularly regarding the emergence of copper-based metallization [13]. In addition, accounting for kerf losses during wafer manufacturing is essential to obtain more realistic estimates of Si demand. While kerf recovery technologies exist on a laboratory and pilot scale, kerf losses remain largely unrecovered in current industrial practice, resulting in significant material loss [38], [39], [40]. Another study by Li et al. (2025) combined the Global Change Assessment Model with material flow analysis to project PV waste generation across 32 global regions under multiple climate ambition scenarios [41]. The results show that global PV waste is expected to surge around 2045, with the total capacity of decommissioned panels reaching 2 000-3 000 GWp by 2050, and that ratcheting climate commitments increase waste volumes by 8-19% compared to the baseline. However, the aggregation of all crystalline-silicon technologies into a single inventory is a key limitation, as it excludes indium in transparent conductive oxide (TCO)-based technologies and lacks detailed projections for evolutions in material intensities, which can significantly affect waste mass and resource recovery estimates.

Across these studies, projected material demands vary considerably depending on the assumed technology mix, deployment scale, and model parameterization. Estimates for cumulative silver demand by 2050 range from below 200 000 metric tons in scenarios with aggressive copper metallization adoption to over 450 000 metric tons under higher silver intensity assumptions [32]. Indium demand projections diverge most sharply: the European Commission study projects an eightfold increase in annual demand by 2030 [6], while Xu et al. project increases of more than 200-fold by 2050 relative to 2022 levels [37], primarily driven by differences in assumed market penetration of SHJ and perovskite-silicon tandem technologies. For bulk materials, projected increases are more consistent across studies, with silicon, aluminum, and copper demand broadly expected to grow two- to twentyfold by 2050, though absolute values differ due to varying assumptions on wafer thickness, kerf losses, and system-level components.

At the regional scale, recent studies have focused on end-of-life (EoL) material flows to evaluate the potential contributions of reuse and recycling to future demand. Kastanaki modeled the effect of circular economy strategies within the EU-27 using a dMFA model, projecting up to 21-35 million tons of PV waste by 2050 [42]. Between 2025-2050, this corresponds to 200-370 ktons of Si, 135-200 ktons of Cu, more than 2 million tons of Al, and 10 ktons of Ag. Furthermore, the study highlights the strong potential for reuse, which could utilize 30-40% of the overall waste stream. For recycling, total Ag mass in waste c-Si panels in 2035 is projected to exceed four times the annual Ag demand in new c-Si panels, with corresponding figures of 23–51% for Al and 12–31% for Cu. However, the model is limited by its reliance on assumed rather than empirically derived material intensities. For China, Liu et al. employed a Bidirectional Long Short-Term Memory (BiLSTM) neural network model to forecast PV installed capacity under three scenarios [43], using Weibull distributions to model the failure probability of PV panels in early and regular loss scenarios. The authors projected that, by 2050 and with a 90% recycling rate, the aggregate weight of recycled PV panels could reach 30%-50% of total PV raw material demand by 2050. While Liu et al. provide a robust forecasting framework for China’s PV waste generation and recycling potential, their analysis treats PV modules largely at aggregate module-level specifications such as area, weight, and efficiency [43]. These studies and others with similar approaches provide valuable insights for forecasting waste volumes and estimating recycling potential. However, they overlook key technology-specific parameters that structurally determine raw material demand, including wafer thickness, kerf losses, metallization loading, and other emerging material substitutions in several components of the PV system. Furthermore, limited differentiation between cell technologies and market share evolution restricts the ability of these studies to capture how design choices influence exposure to critical raw materials.

This report forecasts future raw material demand for the global silicon-based PV sector by extending the parameterized model developed by Xu et al. [37]. The analysis is performed at the system level for c-Si PV technologies and includes material use in the cell, module (encapsulation, backsheet, junction box, and cell interconnection), and balance-of-system (BOS), comprising string inverters, cabling (module-to-module, DC, and AC), and fixed mounting structures. The projected annual inflow of PV systems is then linked to a dMFA model to estimate annual end-of-life (EoL) outflows, their total material mass, and the evolution of in-use stock material content. The modeled cell and module efficiencies, material compositions, and market shares for various silicon-based PV technologies are derived from the 2025 ITRPV projections and extend out to 2035. To explore longer-term implications, the timeframe of this study is extended to 2050, assuming the continuation of trends in market and technology developments. Since this assumption is crude and necessarily further increases uncertainty, a sensitivity analysis is performed to evaluate the range of uncertainty in future raw material demand and to identify the parameters that most strongly influence these outcomes. Finally, resource-use impacts are evaluated using four methods used in the study by Frischknecht & Krebs (2022) [29]. This study reports detailed results for the following materials: Al, Cu, In, Pb, Si, Ag, Au, Sn, and Zinc (Zn). These materials are selected because their mass fractions in

PV systems are specifically parameterized from PV technology roadmap projections and implemented in the dMFA model. Limitations of the current approach are described in the limitations section.

2 MATERIALS AND METHODS

2.1 PV Deployment Scenarios

Global PV deployment has grown significantly, reaching an installed capacity of approximately 2 TWp in 2024 [44]. For future deployment, two main scenarios are defined: a low deployment scenario reaching 29 TW DC capacity by 2050 and a high deployment scenario reaching 63 TW DC Capacity by 2050.

- **Low PV Deployment Scenario (13 TWp by 2035; 29 TWp by 2050)**: This scenario is developed based on the 2024 edition of the IEA NZE scenario [25]. PV deployment is relatively conservative because this scenario achieves net-zero through the deployment of renewables and technologies for CO_2 removal from the atmosphere. As such, the future trend for global installed capacity is assumed to follow exponential growth, increasing from approximately 3 TWp in 2025 to 13 TWp by 2035 (12 TWp in the NZE), and accelerating thereafter to reach 29 TWp by 2050 (22 TWp in the NZE). The higher capacity values relative to the IEA NZE scenario arise from the use of smoothed curve-fitting, as the NZE scenario does not provide year-by-year capacity values. By 2050, PVs could contribute globally to approximately 40% of electricity generation and 25% of total final energy demand [25].
- **High PV Deployment Scenario (17 TWp by 2035; 63 TWp by 2050)**: This scenario is developed based on the results of the energy transition model from the study by Bogdanov et al. (2021) [26]. PV deployment is more optimistic because this scenario achieves net-zero mainly through solar and wind deployment, with no reliance on atmospheric CO_2 removal technologies. As such, global installed silicon-based PV capacity is projected to reach 17 TWp by 2035 (18 TWp in original study with deviations also due to smoothed curve fitting), and 63 TWp by 2050. By 2050, PVs could contribute to approximately 75% of electricity generation and 60% of total final energy demand [26].

For the sensitivity analysis, alternate scenarios with global installed silicon-based PV capacities of 40 and 50 TWp by 2050 are considered to capture the full range of uncertainty in future deployment. A 75 TWp installed-capacity by 2050 scenario is also considered as an exploratory sensitivity scenario based on more optimistic literature assumptions, although it is not derived from an energy transition model [27]. With installed capacity fixed for 2010-2024 and 2050 as boundary conditions, an iterative approach is used to generate a monotonic S-curve growth profile for annual installed capacity. The projected future annual installed capacity for each scenario is summarized in Figure 1.

In the absence of consistent long-term projections for technology-specific deployment in energy transition scenarios, the total projected PV capacity is allocated entirely to c-Si PV technologies in the model. This reflects the current technological dominance of silicon-based PV, which accounts for more than 98% of global PV installations [4]. Non-silicon and thin film PV technologies are therefore not explicitly modeled, as they currently exhibit lower performance and higher manufacturing costs than silicon-based PV and are expected to retain only a limited market share in the future [2], [3], [4], [45]. As such, this assumption may slightly overestimate demand and end-of-life supply for some materials associated with c-Si technologies, while underestimating materials such as tellurium, cadmium, selenium, or gallium.

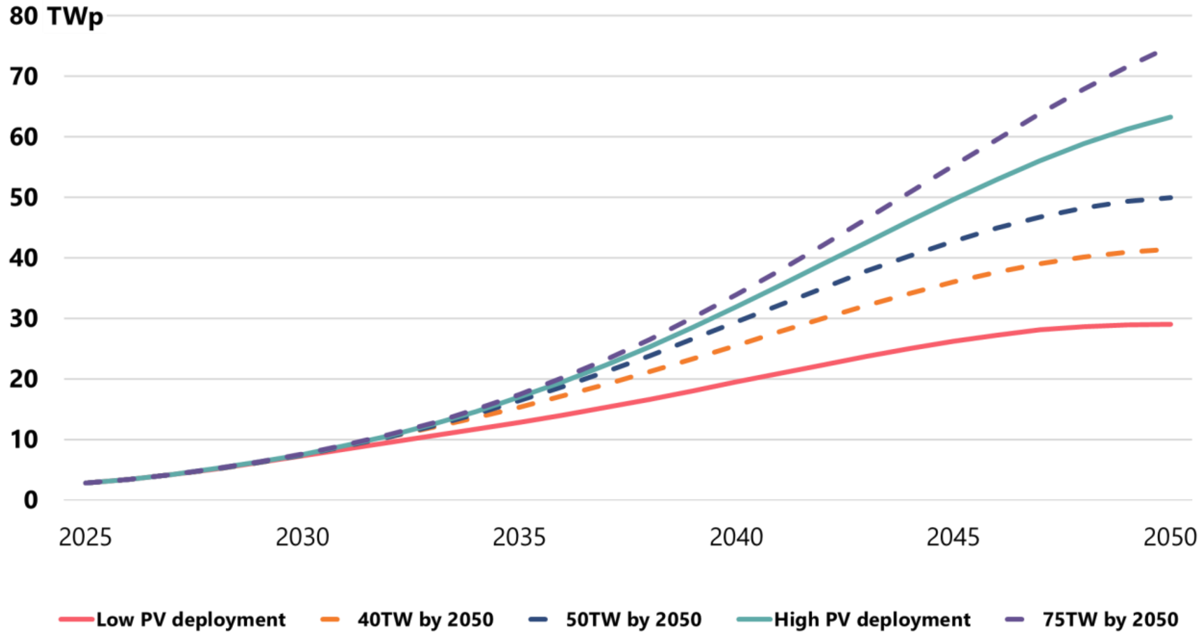

Figure 1: Installed capacity projections for the deployment scenarios presented in this study, including the IEA scenario of 29 TWp by 2050 as low PV deployment [25], and the LUT scenario of 63 TWp by 2050 as high PV deployment [26].

2.2 PV technology developments

This study draws on the ITRPV roadmap for silicon-based PV technologies, including aluminum back surface field (Al-BSF), mainly for sales prior to 2025, as well as PERC, TOPCon, SHJ, interdigitated back contact (IBC), and Pvk-Si-tandem cells for the past and future [13]. In this study, "Pvk-Si-tandem" refers specifically to perovskite-silicon tandem architectures, which are within the scope of this study on c-Si technologies; other tandem concepts, such as perovskite in tandem with copper indium gallium selenide thin-film and single-junction perovskite, are not considered. The roadmap provides detailed projections for efficiency improvements, market share evolution, and material intensities for these technologies until 2035 [25].

As shown in Figure 2, ITRPV projections for technology and market development are extrapolated linearly beyond 2035, with IBCs on SHJ and/or TOPCon cells modeled to dominate due to efficiency gains from the back-contact design. Si-tandem technologies are projected to double their market share between 2035 and 2050, provided that perovskite layers demonstrate adequate stability and durability. To project efficiency improvements, PV technologies are first anchored to their theoretical cell efficiency limits, which are defined as 28.7% for TOPCon, 29.4% for SHJ, and 45.0% for Pvk-Si-tandem technologies [46], [47], [48]. Xu et al. [37] set cell efficiency industry-limits below theoretical efficiencies and assumed constant annual efficiency gains of 0.5% until those limits are reached. However, these are revised in the present work to reflect the accelerated efficiency gains observed in PV technologies between 2022 and 2025. TOPCon is assigned an industrial limit of 28.0% based on recent progress, and SHJ a slightly higher limit of 28.2%. For Pvk-Si-tandems, a 38.0% limit is linearly extrapolated from the widening efficiency gap between SHJ and tandem cells in the

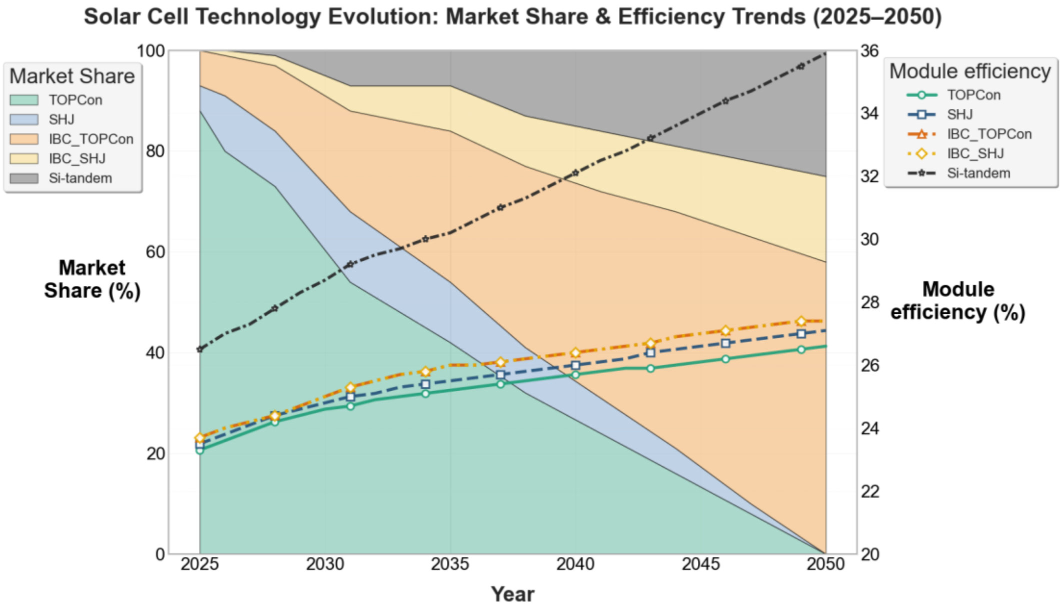

Figure 2: Assumed developments in module efficiency and market share of the different PV technologies

ITRPV 2025 roadmap for the 2025-2035 period. Similarly, IBC cells are assumed to achieve an efficiency gain of 0.5% over front and back contacted cells.

Module efficiencies are derived from the underlying cell efficiencies by applying technology-specific adjustments. For monofacial modules, the module efficiency is estimated to be on average 7.0% lower than the corresponding cell efficiency. This ratio is based on the cell-to-module efficiency values reported in the ITRPV 2025 roadmap for the 2025–2035 period [13]. In the case of bifacial PV modules, the module efficiency is assumed to be 0.5 percentage points higher than that of monofacial counterparts with the same cell technology. Bifacial modules have an estimated market share of 90%, which is projected to increase to 95% by 2035 [13] and is assumed to remain constant afterwards.

The ITRPV report projects an average reduction in wafer thickness from 136 µm in 2024 to 110 µm by 2035. Beyond this point, wafer thickness is assumed to further decrease to an average of 100 µm, with technology-specific values of 90 µm for SHJ bottom wafers in Pvk-Si-tandem cells and 110 µm for IBC cells. Kerf losses, representing material losses during wafer slicing, are estimated based on ITRPV projections. These losses are projected to decline from approximately 53 µm (per total wafer thickness) in 2024 to 42 µm by 2035 [13]. Beyond the ITRPV projection horizon, linear extrapolation to a value of 30 µm by 2050 is performed, consistent with the anticipated direction of continued improvements in diamond wire sawing technology but not tied to a specific published target. Given the inherent uncertainty in this assumption, kerf loss is included as a parameter in the sensitivity analysis presented in Section 2.5, which quantifies its effect on cumulative silicon demand across its expected range.

Regarding Ag intensity in metallization, historical values up to 2023 are taken from the study by Xu et al. [49]. Current technology-specific Ag intensity is estimated at 16.7 mg/Wp for SHJ, 13.6 mg/Wp for TOPCon, and 11.2 mg/Wp for IBC cells, based on ITRPV estimations [13]. Reductions in Ag intensity are assumed to follow ITRPV projections until 2035, where technology-specific Ag intensity reaches 8.1 mg/Wp for SHJ and TOPCon, and 6.5 mg/Wp for IBC cells. Beyond 2035, the "silver optimization scenario" presented in the work of Xu et al. [49] is used to derive estimates for technology specific Ag intensity. According to these estimates, the projected reduction in Ag intensity follows power-law learning curves between 2035 and 2050, amounting to 25% for the low PV deployment scenario and 16% for the high PV deployment scenario. For comparison, Hallam et al. [32] estimated a 20% silver learning curve for the PV sector between 2010 and 2020, demonstrating a quantifiable justification for the projections of this study aligned with current industrial progress.

Cu metallization, including both screen printing and plating technologies, is assumed to increase in market share from 7% in 2024 to 74% by 2035, in line with ITRPV projections [13]. Beyond 2035, the copper substitution scenario of Xu et al. [37] is adopted for market share projections, with Cu screen printing maintaining a dominant market share of approximately 90% and Cu plating accounting for the remainder. Ag intensity projections from the silver optimization scenario are preferred over those from the copper substitution scenario as they are more consistent with ITRPV projections for 2025-2035, while the copper substitution scenario better captures anticipated Cu adoption rates beyond that timeframe.

From the perspective of the PV inflow characterization model, the main difference between the two technologies lies in Ag use: Cu screen printing is assumed to contain a small amount of Ag, ranging from 1.4 to 2.0 mg/Wp [50], while Cu plating is considered silver-free. Another distinction is the cross section of the cell fingers: Cu screen printing is assumed to have a finger cross-sectional area of 1 140 μm² [51], whereas Cu plating is more material-efficient and is assumed to use a reduced cross-section of approximately half that value. Such assumptions will be significantly affected by the conductivity of the Cu fingers. However, given the relatively low market share projected for Cu plating through 2050 in this study and the higher demand for Cu as cabling material, this difference has only a minor influence on cumulative Cu demand, as will be demonstrated in the results section.

At the module level, the market share of glass-glass solar modules is projected to increase from 51% in 2024 to 72% by 2035, based on ITRPV projections [13], and is assumed to further increase linearly to 90% by 2050. The average glass thickness for glass-glass and glass-foil modules is projected to decrease from 2.8 mm (front) and 2.5 mm (rear) in 2025 to 2.6 mm (front) and 2.3 mm (rear) in 2035 [13] to 2.4 mm (front) and 2.2 mm (rear) by 2050. For cell interconnections, lead-containing solder alloys currently hold a market share of 87%, which is projected to decline to 52% by 2035 [13], and is assumed to further decline linearly to 20% by 2050 in line with anticipated regulatory and technological shifts. Frame mass per module is taken from Smith et al. [52] on the basis of a reference mass per square meter of module area and is adjusted over time as module efficiency improves. Aluminum demand for module frames is then derived accordingly and calculated assuming a 97% aluminum mass fraction, typical of aluminum-magnesium alloys [53]. Al currently has a 93% market share in module frames, projected to decline to 80% by 2035 according to ITRPV projections [13], and assumed to decline further to 60% by 2050, based on linear extrapolation of current design trends. This is attributed to wider adoption of alternative frame materials, such as composite materials or stainless steel and frameless module designs.

At the system level, the current market share split between utility and residential-scale installations is 85% and 15%, respectively [54]. For modeling simplicity, this classification assumes that commercial, industrial, and off-grid installations are also classified as utility-scale due to their comparable inverter sizes and junction box configurations, and despite potential differences in balance-of-system design. Beyond 2025, the share of utility-scale installations is assumed to reach 90% by 2030 and maintain a 92% share from 2032 onward, in line with DNV projections for utility-scale installations [55]. The raw material demands of inverters, module-to-module cabling, and additional cabling to connect to the grid are derived from an IEA report on the life cycle inventory of PV systems [56], and the study by Aliang [57]. Inverter material composition is derived from two reference system sizes: residential (2.5 kWp) and utility-scale (100 kWp) in a string-based configuration using data from European and global manufacturers. These inventories are converted into material intensities per installed capacity for residential and utility-scale systems and scaled to the specific installation year using an 11% learning curve [58]. The same learning curve approach is applied to cabling, following Aliang [57], with baseline copper consumption for residential (1.25 Mtons/TWp) and utility-scale systems (3.9 Mtons/TWp) taken from Underwood et al. [62].

Furthermore, the raw material demands of mounting systems are based on the study by Xie [59], which applies a ternary classification, i.e. open-ground, flat roof, and slanted roof. The material intensity of mounting systems is assumed to follow a 2.6% learning curve, with aluminum mounting systems accounting for 75% of the market and steel for the remainder, based on data from ecoinvent datasets as used in the study by Xie [59]. In addition to tracking systems, several BOS components are not explicitly modeled in this study, including pile foundations, floating structures, auxiliary monitoring and control systems, fire protection devices, and battery storage systems. As a result, the projected raw material demand for silicon-based PV systems presented here should be interpreted as an underestimation of overall BOS-related material requirements.

2.3 PV technology functional layer configurations and the underlying material demand

The functional layer configurations for the PV cell technologies considered in this study are primarily derived from literature sources that present life cycle inventories for these technologies [52], [60], [61], [62], [63]. Assumptions for the silicon wafer and the additional functional layers modeled are listed in Table 2-1. **A detailed breakdown of material inputs for each PV system component is provided in Appendix A, including:**

- **a.** Si, Al, In, Sn, Zn, Pb, Ag, and Cu at the cell level
- b. Cu, Pb, Sn, Al, Glass, and plastics (encapsulants, sealants, and backsheet) at the module level
- c. Al, Cu, Ag, Zn, Pb, Au, nickel, steel, manganese, magnesium, titanium, and tantalum at the system level.

Furthermore, the modeling of mono- and bifacial systems assumes that both share the same functional layers and thickness assumptions for each silicon cell technology outlined in Table 2-1. The higher efficiency of bifacial modules results in differences in specific mass at the cell and module level through the area-to-capacity ratio (m^2/kWp) . As cell and module efficiencies evolve over time, the bill of materials changes accordingly. Therefore, Tables A-1 and A-2 which list the specific mass-based material inventories for 1 kWp monofacial and bifacial systems, respectively, are limited to the year 2025 as the starting point.

Table 2-1: Overview of the functional layers and corresponding thickness assumptions per silicon PV cell technology.

Layer	Material	Thickness
PERC		
Silicon Wafer (substrate)	p-type Silicon	*parameterized*
Rear surface passivation	Aluminum Oxide (Al_2O_3)	**10 nm**
Dielectric capping	Silicon Nitride (SiN_x)	**75 nm**

Layer	Material	Thickness
TOPCon		
Silicon Wafer (substrate)	n-type Silicon	*parameterized*
Tunnel oxide	Silicon Dioxide (SiO_2)	**1.5 nm**
Surface passivation	Doped poly-Si	**140 nm**
SHJ		
Silicon Wafer (substrate)	n-type Silicon	*parameterized*
Selective contacts	Amorphous silicon	**30 nm**
Front and back TCOs	Indium tin oxide (ITO)	**130 nm** (80 nm top, 50 nm bottom)
IBC		
IBC cells use similar materials to TOPCon or SHJ but with a different structural arrangement where both positive and negative contacts are located on the back side		
Pvk-Si-tandem		
Bottom cell	SHJ	
Perovskite top cell	Perovskite absorber	**570 nm**
	TCO- Indium Zinc Oxide	**90 nm**
	Electron transport layer- Tin Oxide (SnO_2)	**10 nm**
	Electron transport layer-C_{60} (Fullerene)	**23 nm**

Several categories of materials are excluded from the technology bill of materials. First, abundant elements such as oxygen and nitrogen, which are contained in compounds like SiO_2 and SiN_x layers are excluded, as their availability poses no material constraint. Second, p- and n-type silicon dopant materials (for example boron, phosphorus, and gallium) are also excluded due to their dilute concentrations relative to the total bill of materials. The concentration of dopant atoms in crystalline silicon typically ranges from approximately one dopant atom per billion silicon atoms in lightly doped wafers to about one per 10 000 silicon atoms in heavily doped regions, corresponding to mass fractions several orders of magnitude lower than that of silicon and other cell materials [64]. Mounting hardware and module frame materials other than Al such as galvanized steel rails are also excluded due to the absence of reasonable estimates.

2.4 Material flow analysis model

A dMFA model is developed with the open-source “ODYM” Python framework [65] to estimate material demand for new silicon-based PV installations, the secondary supply of raw materials from EoL systems, and the total material mass locked in in-use stocks. The model is stock-driven because future PV deployment is defined in terms of future installed capacity, which represent the in-use stock of PV systems. Annual material demand and end-of-life outflows are derived from this stock evolution and lifetime assumptions. The PV stock and flow dynamics are governed by the following balance equation:

$$S[t] = S[t-1] + I[t] - Q[t] \qquad (1)$$

where $S[t]$ is the in-use PV stock in year t (TWp), $I[t]$ is the annual inflow (new installations), and $Q[t]$ is the annual outflow of decommissioned PV modules.

This study takes a stock-driven approach by using global silicon-based PV capacity projections to estimate material demand. The annual inflow of new capacity is determined by both the targeted stock size and the lifetime of PV systems, since product longevity governs the timing and magnitude of EoL outflows. As such, the annual input flow of new capacity, $I[t]$, is calculated as the difference between the stock in year t and the previous year, plus the outflow due to decommissioning:

$$I[t] = S[t] - S[t-1] + Q[t] \qquad (2)$$

The outflow is modeled using a convolution with a probabilistic lifetime distribution that predicts module retirement:

$$Q[t] = \sum_{t'=2010}^{t-1} I(t-t') \cdot P(t-t') \qquad (3)$$

where $P(t-t')$ is the probability of module retirement at age $(t-t')$, with t' being the year of deployment. Material demand and secondary supply are then calculated based on the stock and technology-specific material intensities:

$$M_{in,j}[t] = I[t] \cdot m_j[t] \qquad (4)$$

$$M_{out,j}[t] = \sum_{t'=2010}^{t-1} I(t-t') \cdot m_j(t-t') \cdot P(t-t') \qquad (5)$$

where $M_{in,j}[t]$ is the inflow (kg) of material j in year t, $M_{out,j}$ is the outflow (kg), and m_j is its corresponding material intensity in year t (kg/TWp). The study assumes full collection and 100% recycling efficiency to estimate an upper-bound potential. To avoid adding highly uncertain assumptions, the study does not model collection losses, processing inefficiencies, and material contamination are excluded from the system boundary. Incorporating these factors would require speculative assumptions in the absence of globally consistent data.

Material intensities for module-level components (e.g., glass, frame), BOS elements (inverters, cabling, mounting structures), and certain materials used at the cell level (e.g., Ag and Cu screen or plated contacts) are directly estimated as input intensities expressed in kg/kWp. In contrast, the intensities of other cell-layer materials (e.g., silicon wafer, passivation layers, TCOs, and additional functional coatings) are calculated dynamically as a function of module efficiency, technology-specific market share, and layer thickness, as shown in the equation below:

$$m_j[t] = \sum_i \frac{L - thi_{i,j}[t] \cdot \rho_j \cdot Share_i[t]}{\eta_{mod,i}[t]} \quad (6)$$

where $L - thi_{i,j}$ is the layer thickness of material *j* in technology *i* (m), ρ_j is density of material *j* (kg/m^3), $Share_i$ is the market share of technology *i*, (%), and $\eta_{mod,i}$ is module efficiency of technology *i*, (%). The resulting material intensity is expressed in mass per installed capacity, with units converted consistently across the model to million metric tons per terawatt-peak (Mtons/TWp).

PV lifetimes depend on several factors, including power degradation, technical failures, extreme weather events, and economic considerations. Residential systems are more often influenced by financial incentives to replace older modules, while utility-scale installations typically operate longer due to their capital-intensive nature. Although SHJ modules typically exhibit lower degradation rates than other c-Si technologies, technology-specific lifetimes are not distinguished here due to limited long-term empirical data and are assumed to apply equally to all emerging technologies.

This study uses Weibull distributions to model PV lifetimes, with parameter values drawn from recent literature:

- **Residential PV**:

Based on the "middle-ground" scenario developed by Tan et al. [66], which balances power loss and economic motivation.

Average lifetime: **18 years**

Weibull parameters: shape = 2.5, scale = 20

- **Utility-scale PV**:

Based on the Early Loss scenario from IRENA and IEA-PVPS from the study by Tan et al [66].

Average lifetime: **26 years**

Weibull parameters: shape = 2.5, scale = 30

To describe long-term trends in PV deployment and associated material demand, the compound annual growth rate (CAGR) is used. CAGR provides the smoothed annual rate of growth over a specified period and is calculated as shown in equation 7.

$$CAGR = \left(\frac{V_{fin}}{V_{ini}}\right)^{1/t} - 1 \quad (7)$$

where V_{fin} is the final value, V_{ini} is the initial value, and t is the number of years. Furthermore, based on the 5 deployment scenarios presented in section 2.1, a set of results are presented for the total material mass of in-use stock, inflow, and outflow streams based on the outcomes of those 5 deployment scenarios.

2.5 Sensitivity analysis

A one-at-a-time (OAT) sensitivity analysis approach is performed to evaluate the standalone effect of specific technical parameters on cumulative raw material demand, independent of the scale of future deployment. Parameters are selected based on two primary criteria:

a. a direct link to the demand of a specific material, such as the relationship between wafer thickness and silicon demand, silver metallization intensity, and the market penetration of indium-based PV technologies.
b. the presence of significant future uncertainty.

As such, parameters that affect all materials uniformly, such as future cell and module efficiency gains, are excluded because their effect on material demand is directly captured through the material intensity formulation, where demand scales inversely with module efficiency, as shown in equation 6. The parameters included in the sensitivity analysis are those whose influence on material demand is less straightforward, involving intermediate assumptions about technology market shares, process-specific loss factors, or learning curve dynamics, where quantifying these relationships represents a methodological contribution of this study. The parameters investigated in this sensitivity analysis are listed in Table 2-2, each tested across the range of values already defined in Sections 2.1 and 2.2. Where the PV technology roadmap [13] explicitly defines intermediate values between 2025 and 2035, as for wafer thickness, kerf loss, and silver paste loading, these are used directly. For other parameters, values are interpolated between the assumed start and end points.

For each iteration in the OAT sensitivity analysis, a single parameter is held constant at one of the fixed values listed in Table 2-2 for the entire 2025-2050 period. All other parameters keep their baseline year-to-year values that were established in Sections 2.1 and 2.2. Then, the cumulative demand for the relevant raw material under investigation is recalculated across the five deployment scenarios outlined in Section 2.1. The resulting difference from the baseline cumulative demand is interpreted as a measure of the sensitivity of the model to that parameter. A limitation of this approach is that it does not explicitly model interactions between parameters and with other parameters not included in this sensitivity analysis framework, which could be the subject of future research.

Table 2-2: Uncertainties considered in the sensitivity analysis and the values assumed

	Values assumed	Unit
Silicon		
Wafer thickness	[90, 100, 112, 117, 124, 136]	µm
Kerf loss	[30, 42, 45, 49, 53]	µm
Silver		
Silver screen printing, silver paste loading	[4, 8, 12, 16]	mg/W
Market share of silver screen printing	[0, 20, 40, 60, 80, 100]	%
Indium		
Market share of technologies containing ITO layers	[5, 20, 45, 70]	%
Copper		
Learning curve for inverters and cabling	[5, 11, 15]	%
Aluminum		
Market share of aluminum as module frame material	[40, 60, 75, 90]	%

2.6 Resource-use assessment

While quantifying absolute material demand is essential for guiding investments in the mining sector and identifying technologies and deployment scenarios with lower material intensity, it does not account for the relative scarcity or potential supply disruptions of those materials. To complement this perspective, the four impact category indicators recommended or suggested by the Life Cycle Initiative hosted at UN Environment for assessing resource use of silicon-based PV systems, as was done in the work of Frischknecht & Krebs (2022) [29] are used:

a. resource depletion with the Abiotic Depletion Potential, ultimate reserves (ADP_{UR}) [67]
b. economic resource scarcity with the Abiotic Depletion Potential, economic reserves (ADP_{ER}) [67]
c. resource quality with the Surplus Ore Potential, Ultimate Recoverable Resources (SOP_{URR}) [68],
d. resource criticality with the Integrated Method to Assess Resource-Use Efficiency (ESSENZ method) [69], [70].

The results of the two versions of the ADP method are normalized and expressed relative to antimony, resulting in a final unit of Megatons of antimony equivalents (Mtons Sb eq.). Antimony is selected as the reference material in the ADP method, though its choice is arbitrary and does not affect relative comparisons [67]. Furthermore, the SOP_{URR} method evaluates the relative consequences of the contribution of a product system to changing resource quality using log-logistic relationship between ore grades and cumulative extraction [68]. For this method, the characterization factor of antimony is also used as a reference for all raw materials investigated to covert results to a final unit of Mtons Sb eq., as shown in equation 8.

$$SOP_{URR}^{norm} = \sum_i \frac{m_i \cdot CF_i}{CF_{Sb}} \quad (8)$$

Where m_i is the cumulative mass of resource *i*, CF_i is the SOP_{URR} characterization factor derived from the log-logistic ore grade-cumulative extraction relationship, and CF_{Sb} is the SOP_{URR} characterization factor of antimony.

In addition to geological availability, criticality assessments of raw materials take into consideration broader geopolitical and market-related risks such as supply concentration or restrictive trade policies [71]. Therefore, the criticality characterization factors of the ESSENZ method are used [69]. They comprise 10 impact categories which measure several supply risk and economic importance aspects related to the primary production of raw materials [70]. Similar to the SOP_{URR} method, for each raw material, the 10 characterization factors are summed and normalized relative to antimony, resulting in a final unit of Mtons Sb eq. Additionally, for all methods used in resource-use assessment, the calculations are done for the entire demand, which provides an upper-bound estimate of the resource-use impacts of the global silicon-based PV sector.

For clarification, the projected raw material demand by the silicon-based PV sector is compared to the global reserves, and for indium specifically will be compared to the global reserves and resources combined. The study adopts the taxonomy from the Mineral Commodity Summaries report issued by the U.S. Geological Survey [7], which defines reserves as: "That part of the reserve base that could be economically extracted or produced at the time of determination." For resources, the study which provides the global indium resource estimate defines resource as "Resources of a particular material are larger than reserves in that resources represent material that is known with some degree of certainty to exist in the crust and might be technically, legally, and commercially viable to produce under some conceivable circumstances." [14]. However, the ADP method defines ultimate reserves as the global crustal content of a certain material [67]. To avoid confusion, this study consistently follows the USGS taxonomy when interpreting reserve limits for most PV raw materials, combined reserves and resource estimate for indium, and explicitly distinguishes these from ADP-based definitions.

3 RESULTS AND DISCUSSION

3.1 Future demand trends and recycling prospects for PV materials

Figure 3 presents the total mass of the global in-use stock, EoL outflows, and new additions of silicon-based PV systems for the two main deployment scenarios introduced in Section 2.1. The corresponding results expressed in terms of stock capacity are presented in Figure 4. Differences in in-use stock mass from the two scenarios become noticeable after 2035. By 2050, the in-use stock mass in the high-deployment scenario is more than double that of the low-deployment scenario. The dMFA model further projects that new annual installations could peak between 2040 and 2045, reaching approximately 1.7 TWp in the low deployment scenario and 4.1 TWp in the high deployment scenario. This peak is driven primarily by the continued expansion of global silicon-based PV installed capacity, as shown by the corresponding peaks in annual material demand in Figure 3 (c-d).

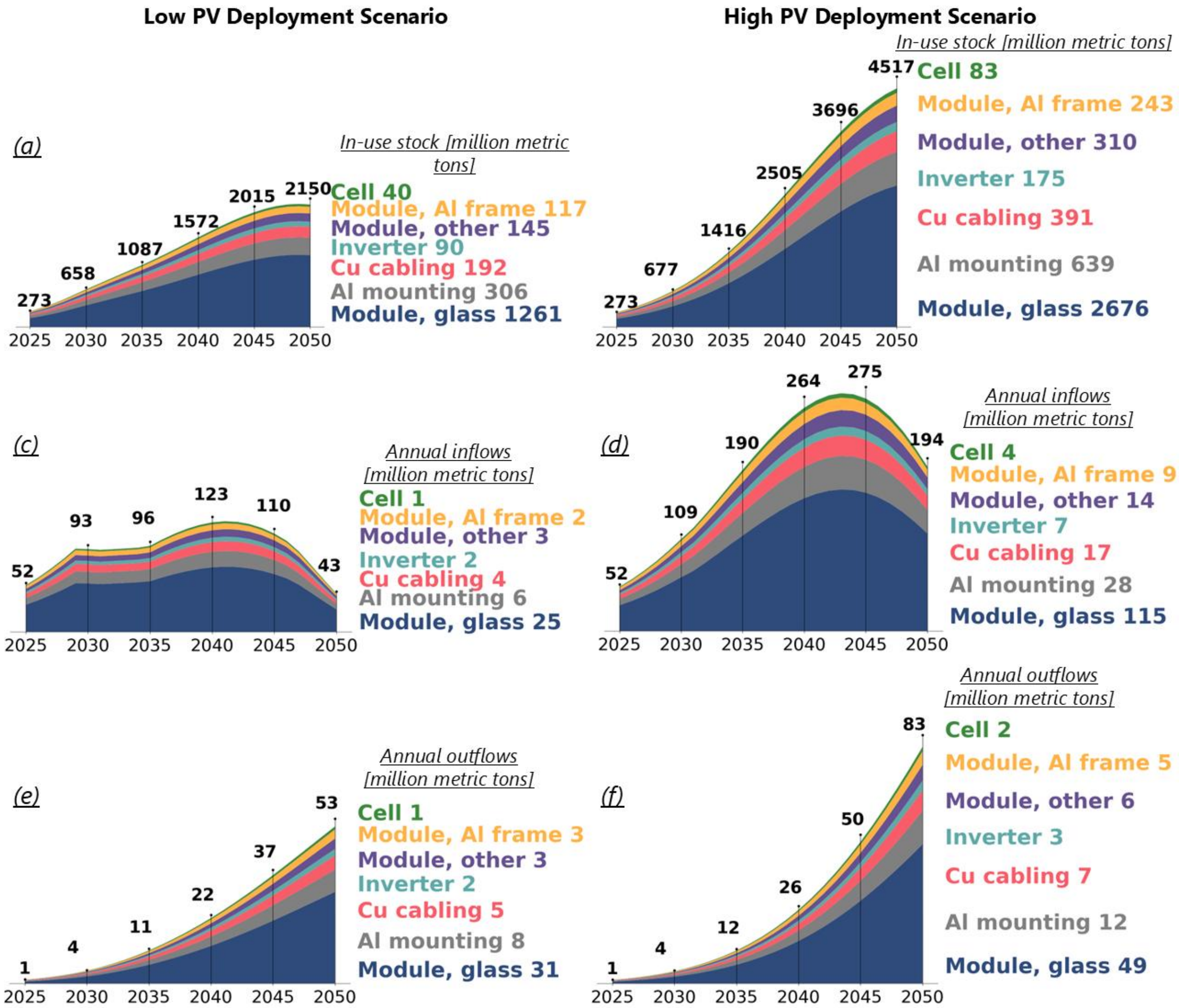

Figure 3: (a,b) material breakdown of in-use stock mass of global PV installed capacity, (c,d) breakdown of annual inflow mass, (e,f) breakdown of annual outflow mass (million metric tons). (a,c,e) correspond to the low PV deployment scenario, (b,d,f) correspond to the high PV deployment scenario.

The replacement of PV systems reaching their EoL contributes to new installations as well, but to a lesser extent, as annual outflow masses remain smaller than annual inflows during this period (Figure 3 (e-f)). After 2045, new annual installations decline as the growth rate of installed capacity flattens in the later stages of the deployment trajectory, leading to lower incremental capacity additions over time (Figure 3 (c-d)). As highlighted in previous studies [66], [72], an increasing number of PV systems are reaching their EoL earlier than their expected technical lifetime due to external factors such as extreme weather event damage, installation failures, or component degradation. Economic factors are also incentivizing the premature replacement of functioning systems, further contributing to higher EoL volumes. Such nuances could be considered in more detail in future studies.

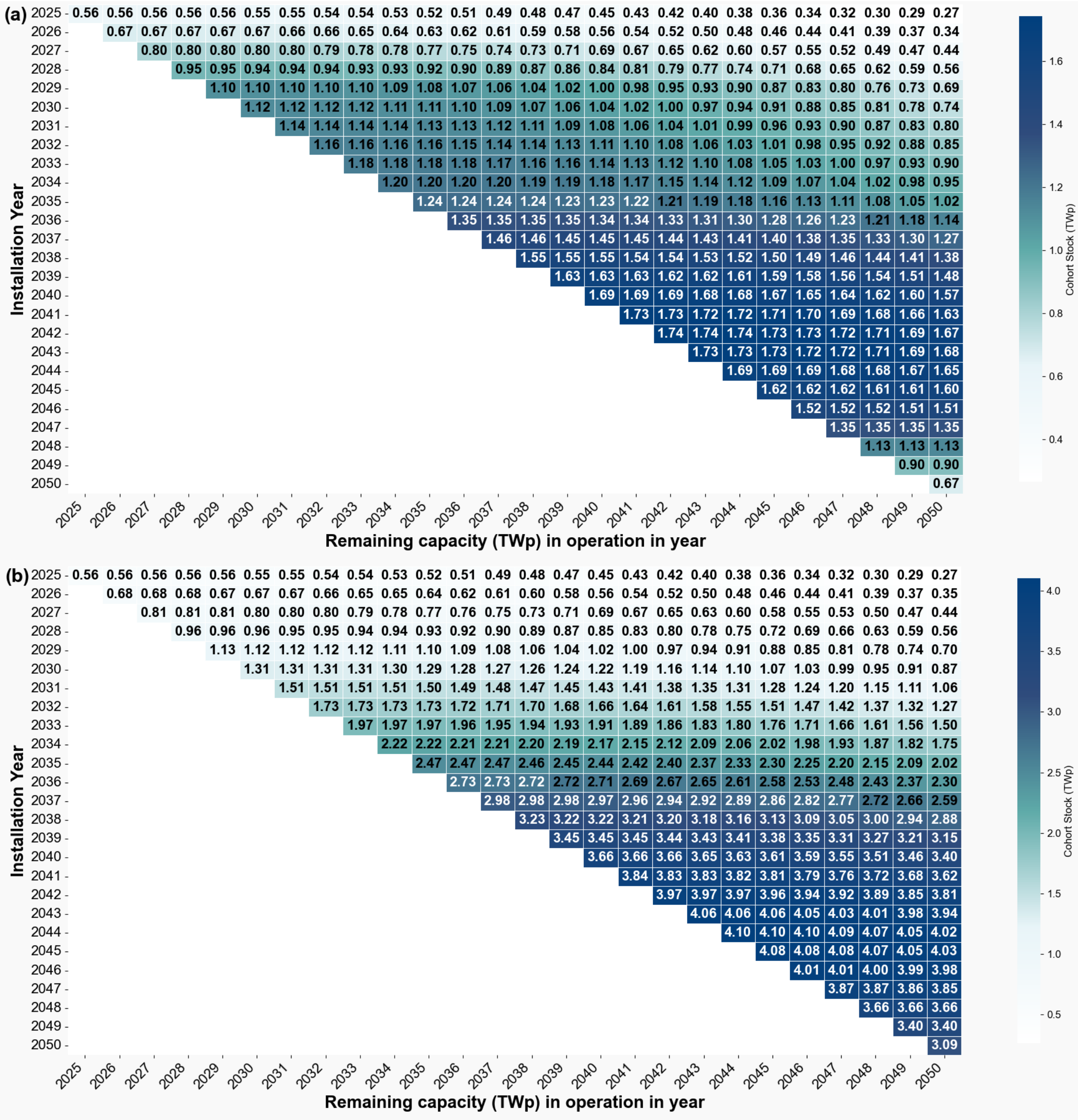

Figure 4: Cohorts of in-use PV stock (TWp) by installation year and remaining deployment years. (a) low PV deployment scenario, (b) high PV deployment scenario. The leftmost column represents annual new installations for each installation year, while subsequent values in each row track the decline in remaining capacity over time due to end-of-life outflows.

Results from Figure 3 indicate that the annual EoL flows are about 57% higher in the high deployment scenario than in the low deployment scenario by 2050, despite a 110% difference in in-use stock. This smaller difference in waste flow estimates is primarily due to the long lifetime of PV systems, which slows the growth of the waste stream and results in a continuous accumulation of in-use stock over time. **Given the limited variation in waste stream estimates up to 2040, the model projects cumulative end-of-life outflows of more than 15 million metric tons of silicon-based PV systems between 2025 and 2030, increasing rapidly to approximately 131 million metric tons between 2030 and 2040.** Of this cumulative EoL mass, modules account for around 71 weight percent (w%), while BOS components account for the remaining 29w%, based on the system-level bill of materials used in the model (Sections 2.2, 2.3, and Appendix B). Detailed results for annual EoL outflows in GWp and the in-use stock mass of key materials are presented in Appendices C and D, respectively.

As shown in Figure 3 (a-b), glass accounts for the largest share of materials in the in-use PV stock (59w%), followed by aluminum used in mounting structures module frames, and inverters (21w%) in line with the findings of Kastanaki [42]. Cell materials, mainly Si, contribute only marginally, representing approximately 2w% of both the in-use stock and the waste stream. For the in-use stock in 2025, the average front glass and back glass thicknesses are estimated at 2.9 and 2.4 mm, respectively. The results of the dMFA model based on developments in cell and module manufacturing presented in Section 2.2 show that in 2050, these thicknesses are modeled to be reduced to an average 2.5 and 2.3 mm for the whole in-use stock. Similarly, average silicon intensity in wafers within the in-use stock is projected to decline from 2.2 kg/kWp to 1.3 kg/kWp (a reduction of more than 40%). Steel, composites, plastics, and frameless designs are gradually replacing Al as frame materials [13]. As a result, the share of Al frames in the in-use stock total mass is expected to fall from 6.4w% in 2025 to 5.4w% by 2050. **The anticipated increase in resource-use efficiency of PV manufacturing processes, long product lifetimes, and material substitutions could ultimately contribute to a slowing or even a decrease in annual raw material demand by 2050, which will addressed in Figure 7 and the related discussion**.

Figure 5 illustrates cumulative Cu demand in the PV sector, which is expected to increase significantly over the timeframe of the study mainly due to the expansion of installed capacity. Total Cu in-use stock is projected to increase from approximately 20 Mtons in 2025 to 130 Mtons by 2050 for low PV deployment and 250 Mtons for high PV deployment.

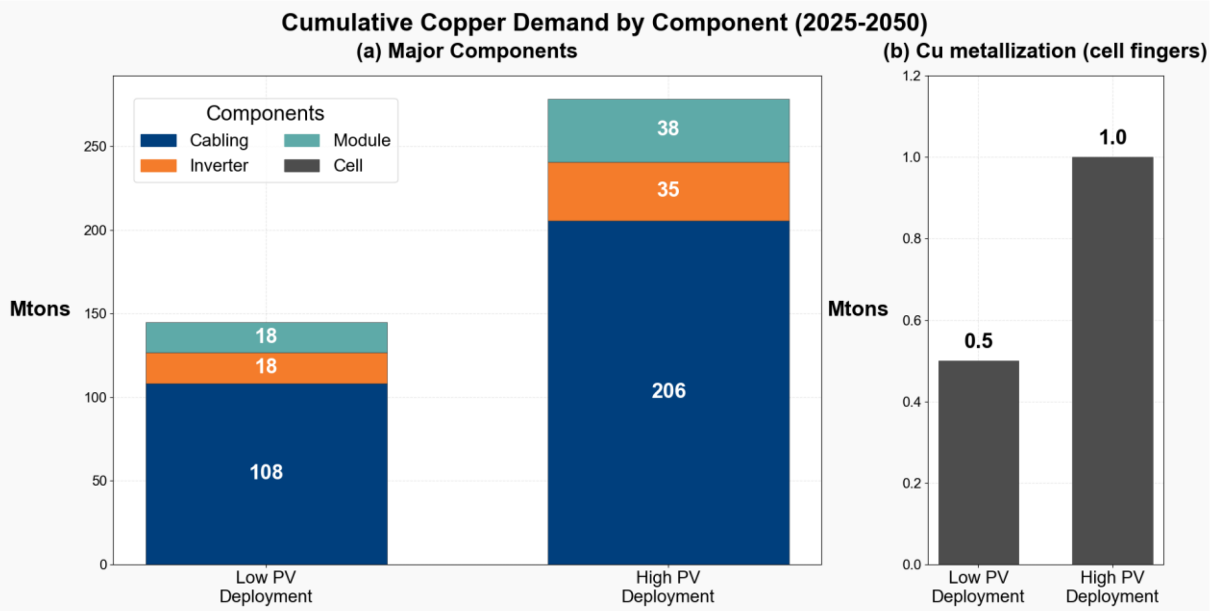

Figure 5: Forecasted cumulative Cu demand by PV system component (2025-2050). (a) cumulative demand for module (cell interconnections), inverters, & cables (b) cumulative demand for cell metallization

Cables are the main PV component driving demand for Cu, accounting for 75w% of the total Cu stock, followed by inverters at 13w%. While the fraction of total Cu used in interconnect ribbons remains relatively low with respect to cables and inverters, its mass fraction in PV system is expected to decrease by more than 20% based on the module efficiency assumptions presented in section 2.2.

While Cu use per kWp in metallization is projected to increase due to the gradual substitution of silver with copper-based pastes, this increase is about 0.3w% of the total copper demand for the global silicon-based PV installations. As such, it is insignificant compared to the overall increase in system sizes and the associated demand for cabling, particularly in utility installations. **By 2050, Cu mass in annual EoL outflows is expected to reach approximately 3 Mtons/year under a low deployment scenario and 5 Mtons/year under a high deployment scenario**. A substantial share of this waste arises from cabling and inverter components with high potential for recovery in recycling processes. Under an ideal closed-loop recycling assumption, Cu recovered from annual EoL outflows could supply about 45w% to 100w% of annual PV-sector Cu demand by 2050, depending on the scale of new installations, as shown in Figure D-2 in Appendix D. In practice, Cu recovery from cables may be limited by complex cable insulation, diverse cable configurations, and high dismantling costs [73]. Furthermore, lead in solder alloys on cell interconnectors may complicate Cu recovery, requiring additional treatment and potentially reducing recovery rates [17].

In Figure 6, cumulative Al demand across all PV components is projected to exceed 500 Mtons between 2025 and 2050 under the low PV deployment scenario**, driven primarily by the material intensity of mounting structures, which account for nearly 70w% of the cumulative demand, and module frames, which account for more than 25w%**. For the high deployment scenario, cumulative Al demand may even exceed 1 Gtons by 2050, with an in-use stock of approximately 920 Mtons in the same year. From Figure D-2, Al mass in EoL outflows is estimated to reach approximately 11 Mtons/year by 2050 under low deployment, and 17 Mtons/year under high deployment. Depending on the scale of future annual installations, Al mass fraction in the annual EoL outflows could be equivalent to 45w% to the

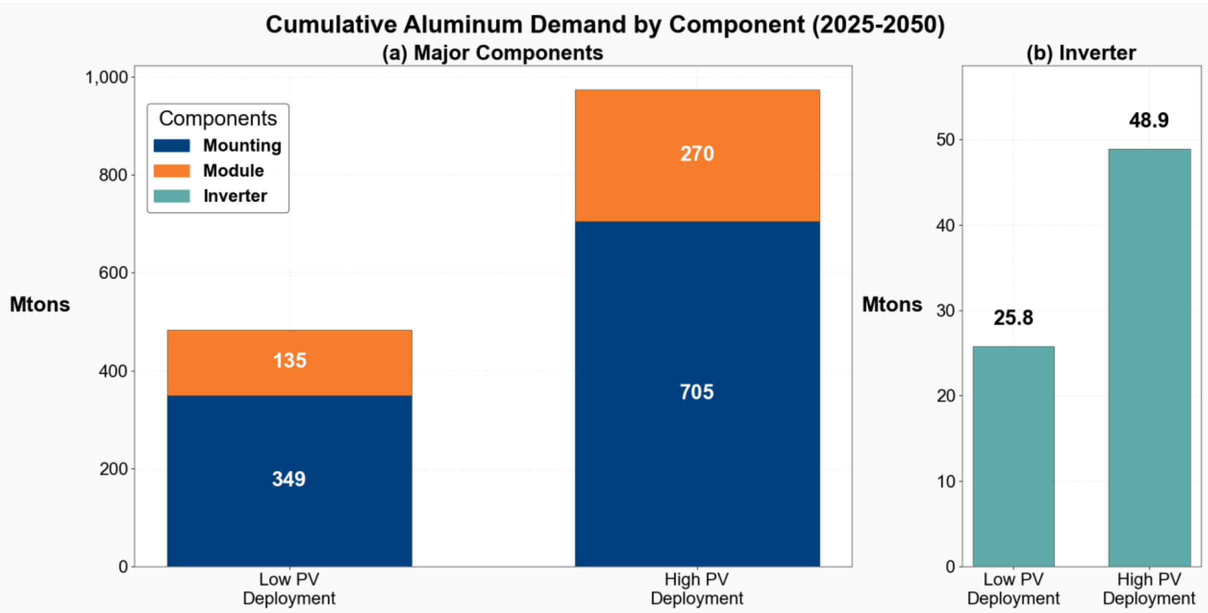

Figure 6: Forecasted cumulative Al demand by PV system component (2025-2050). (a) cumulative demand for module (frame) & mounting structure (b) cumulative demand for inverter

full annual demand of the PV sector by 2050. In practice, however, several constraints limit the potential of closed-loop recycling of Al from PV systems. One key constraint is the need to dilute and cascade scrap with higher-grade aluminum to achieve the required alloy composition [74]. This is particularly relevant for PV module frames, which rely on extruded wrought alloys (aluminum-silicon-magnesium class) that are highly sensitive to impurities [75]. Moreover, Al for rear contacts and antireflection coating layers have minimal contributions (<0.01%) to the total demand and are thus not shown in Figure 6, but considered in the model.

As shown in Figure 7(g), Si contained in future silicon-based PV waste stream **may only marginally contribute to meeting future silicon demand through closed-loop recycling within the modeled period to 2050.** Based on the projected annual demand from the dMFA model under the assumed evolution of installed capacity, wafer thickness, and kerf losses, solar-grade Si annual demand may grow at a CAGR of 5-10% between 2025 and 2040, followed by a downward trend of -10% for low deployment and -3% for high deployment until 2050. Despite accounting for anticipated reduction in kerf losses from the ITRPV study, the dMFA model predicts **significant kerf losses in wafer production throughout the timeframe of this study. In the low PV deployment scenario, total kerf losses are estimated at 15 Mtons, while in the high deployment scenario, this amount doubles to 30 Mtons**.

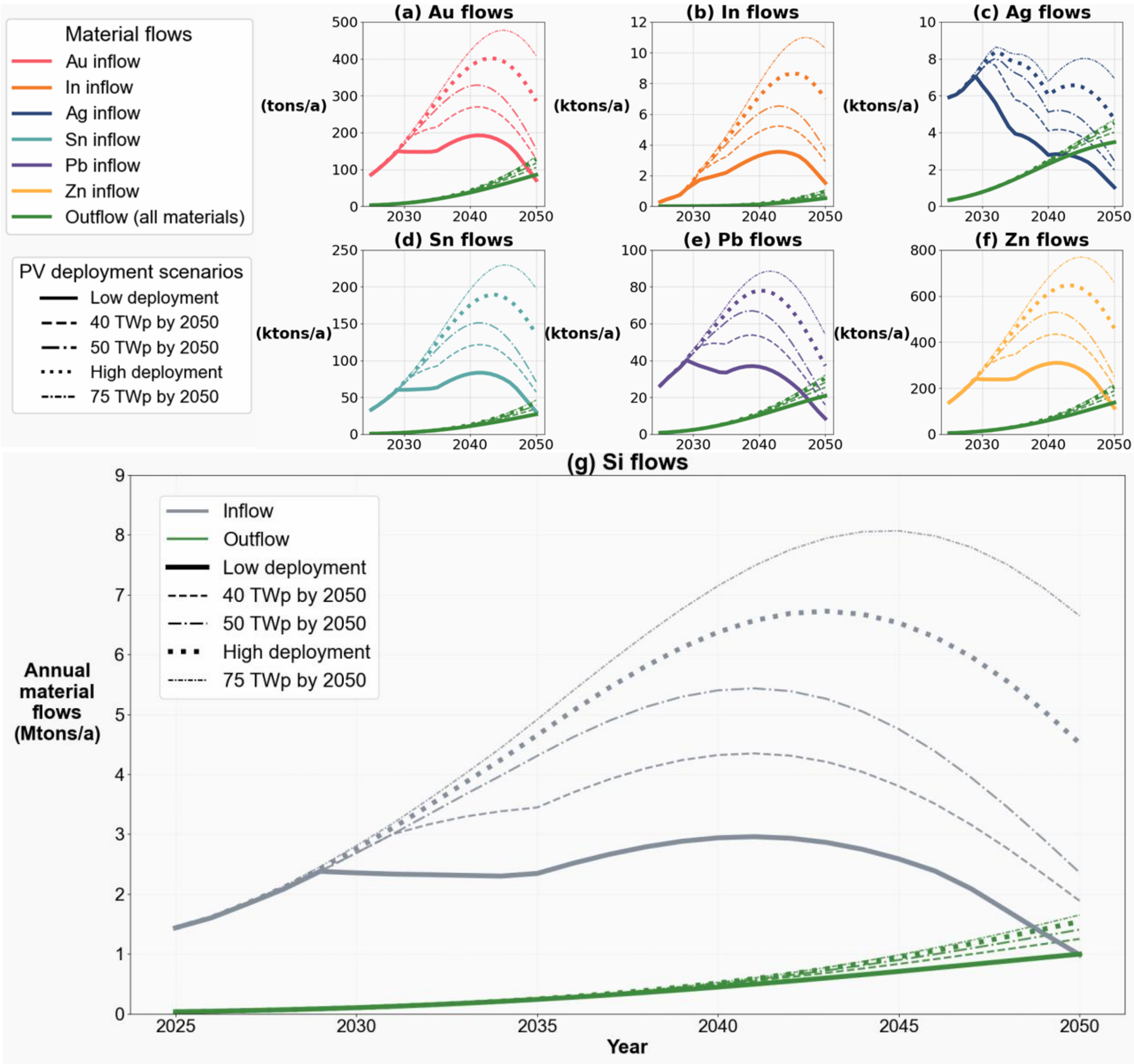

Figure 7: Forecasted annual inflow demand and secondary supply of PV raw materials for the five deployment scenarios. (a) annual gold in- and out-flows, (b) indium, (c) silver, (d) tin, (e) lead, (f) zinc, and (g) silicon

In the low PV deployment scenario, Si recovered from annual EoL outflows could meet an average of 8w% of annual demand between 2025 and 2040. As market demand stabilizes after 2040, this contribution increases noticeably, reaching an **average of 40w%**. In contrast, under the high deployment scenario, the relative contribution of Si in EoL flows remains more modest, **averaging only 18w% beyond 2040** as new installations continue to outpace EoL flows. In practice, recovered silicon from EoL PV systems is assumed to be metallurgical grade and typically contains impurities introduced during cell fabrication, module operation, and recycling, resulting in purity levels that differ from virgin silicon [76], [77]. Because silicon manufacturing requires very strict impurity tolerances, the lack of comprehensive and reliable impurity characterization, combined with the cost of additional purification, remains a major barrier to large-scale reuse of recovered silicon in high-purity applications [76].

Indium is another PV raw material in which future PV waste streams **could marginally meet future demand through closed-loop recycling**, as shown in Figure 7(b). Remarkably, annual demand exhibits a CAGR of 18-24% until 2040 due to the increasing market share of SHJ and Pvk-Si-tandem technologies. These technologies are assumed to gain significant market share at a relatively later stage compared to more established technologies such as TOPCon. As a result, most indium-containing PV systems are modeled to be in use at the end of the study period, with In mass in EoL flows only meeting 5w% of cumulative demand, as shown in Figure D-4(g). In addition, significant In losses during ITO deposition mean that total material demand is approximately twice as high as the embodied indium requirements in finished modules [55]. While some recovery of manufacturing scrap is technically feasible [78], [79], it is not explicitly modeled in this study. ITO losses during deposition are assumed to decrease from 50 percent in 2025 to 40 percent in 2050, reflecting anticipated improvements in deposition efficiency [80], [81], [82]. However, theoretical and industrial estimates of indium consumption for ITO (and recovery potential) in SHJ cells vary widely, largely due to differences in how deposition-related losses are accounted for (e.g., material deposited on chamber components and incomplete sputter target utilization) [30]. In the low PV deployment scenario, **cumulative 2025-2050 In demand is projected to exceed global reserves and resources by 2046 (estimated at 50 ktons [14]). In the high deployment scenario, this threshold is already surpassed by 2040.** In contrast, the cumulative EoL flows between 2025 and 2050 may only contain 4 ktons of In under the low deployment scenario and 6 ktons under the high deployment scenario. By 2050, the in-use stock of In may reach nearly 72 ktons in the high deployment scenario, compared to 30 ktons in the low deployment scenario, as shown in Figure D-1(b) in Appendix D.

The results presented in Figure 7(c) show that **Ag in future PV waste streams has strong potential to meet future demand through closed-loop recycling after 2040. This is driven primarily by increased copper substitution in cell metallization, along with the more efficient use of thinner cell fingers [13], which reduces material intensity and also increases cell efficiency due to reduced shading**. However, this represents a challenge for recycling processes as Ag contributes to roughly half of the value recovered from a recycled PV module [77]. Furthermore, mechanical recycling, which remains the benchmark technology, yields outputs of insufficient purity, and improving silver recovery rates is essential for both economic and environmental performance [17]. Until 2030, annual Ag demand is projected to increase at a CAGR of approximately 2% and 5% under low and high PV deployment scenarios, respectively. This increase is driven by increased new installations, which outpace reductions in Ag intensity. Between 2030 and 2050, however, Ag annual demand is expected to decline, with negative CAGRs of -9% and -3%, driven by the widespread adoption of Cu metallization and the stabilization of new installations**.** As shown in Figure D-1(c)**, in-use Ag stock is estimated at 90 ktons and 150 ktons by 2050 under the low and high deployment scenarios, respectively**. In the low deployment case, the in-use stock total mass of Ag begins to decline after 2043. This decline is driven by a dual effect: (i) decreasing Ag concentrations in new installations added to the stock, and (ii) a growing outflow of older PV systems with higher Ag concentrations. In contrast, under the high deployment scenario, the in-use stock does not decline but instead stabilizes, as new installations continue to offset reductions in per-unit silver use and compensate for the retirement of older, silver-rich PV systems.

Pb in the future waste stream **has high potential to meet future demand through closed-loop recycling, largely due to the ongoing substitution of lead-containing solder alloys in PV module manufacturing** [13]**,** as shown in Figure 7(e). With proven technical feasibility for both physical and chemical separation processes [83], [84], approximately 230-300 ktons of Pb could theoretically be recovered from the waste stream. However, realizing this as closed-loop supply to the PV sector would require sufficient collection infrastructure, competitive recovery economics, and coordination with other industries that also process lead-containing waste streams. Until 2040, annual demand for Pb is projected to grow at a CAGR of approximately 2% under the low deployment scenario and 7% under the high deployment scenario. However, beyond 2040, this trend reverses. As market demand stabilizes and the transition away from lead-based solder alloys accelerates, Pb demand begins to decline, with a negative CAGR of -15% for the low deployment scenario and -8% for the high deployment scenario between 2040 and 2050. From Figure D-4(i), the cumulative Pb demand between 2025 and 2050 is expected to range between 0.8 and 1.5 Mtons, depending on the deployment trajectory.

Similar trends are observed for the future demand and secondary supply of **Au**, **Sn**, and **Zn**, which are illustrated in Figure 7(a-d-f), respectively. Au, which is used in small quantities in inverter electronics, has a substantial cumulative demand between 4-7 ktons between 2025 and 2050 for the five deployment scenarios, the average of which is equivalent to 10w% the global reserves estimate in 2024 [7]. Closed-loop recycling of Au in the cumulative waste stream generated in the same period can only match 15w%-23w% of the demand. For Sn, demand is primarily driven by solder alloys, with minor contributions from content in inverters and ITO layers. Its cumulative demand between 2025 and 2050 could amount to 38w%-78w% of the estimated global Sn reserves reported in 2024 [7], depending on the deployment scenario. In the high deployment scenario, peak annual demand for Sn is projected to occur around 2043 and could reach up to 65w% of global annual mine production in 2024 [7]. The model projects annual outflows Sn content to be equivalent to 30w%-90w% of annual demand by 2050. For Zn, cumulative demand between 2025 and 2050 is projected to range from 6-12 Mtons (in function of future installed capacity), with approximately 90w% of that quantity expected to be embedded in the in-use stock by 2050. This cumulative demand is equivalent to 3w%-5w% of the estimated global Zn reserves reported for 2024 [7]. Over the analysis period, Zn demand is dominated by PV inverters, with marginal contributions from IZO layers in Pvk-Si tandem technologies. Zn in outflow PV systems decommissioned between 2025 and 2050 is only equivalent to 15w%-23w% of the total demand, whereas peak annual demand (647 ktons/year) represents 5w% of global annual mine production (as of 2024) [7].

The recycling results presented above represent a theoretical upper bound, as they assume full collection and complete recovery of material fractions. In practice, secondary supply is reduced by collection losses, contamination, and process inefficiencies. Under the EU WEEE Directive [85], collection and recycling targets of 85% and 80% will result in an effective recovery rate of approximately 68% of end-of-life module mass. Applying this factor would reduce the estimated secondary supply by roughly one-third. However, this remains an upper bound estimate itself, as it assumes global compliance with EU targets. In reality, approximately 10% of end-of-life modules worldwide are currently recycled, with the remainder landfilled or informally disposed of [86]. Even within formal recycling streams, non-specialized facilities achieve overall recycling rates of approximately 24% by mass [87].

3.2 Sensitivity analysis

The sensitivity analysis results demonstrate how variations in: (i) future installed silicon-based PV capacity in 2050 and (ii) market or technology development parameters listed in Table 2-2 affect the cumulative demand for raw materials between 2025 and 2050. The results are presented as 3D surface plots in Figure 8, Figure 9, and in the additional results reported in Appendix E. The surface plots demonstrate the range of possible future demands as well as the relative sensitivity to each factor by examining cross-sections of the surface (holding one variable constant while varying the other). This allows for determining whether the raw material demand is more influenced by the scale of future deployment or market/technology developments.

For Ag, the cumulative demand between 2025 and 2050 is projected to range from 50 to 600 ktons, depending primarily on the market share of silver screen printing and, to a much lesser extent, total installed capacity, as shown in Figure 8(a). A lower market share of silver screen printing results in significantly lower Ag demand at any given capacity, which indicates the strong influence of the introduction of Cu-based metallization on Ag future demand. From Figure E-1 in Appendix E, the sensitivity analysis results show that Ag paste loading also has a strong influence, causing future Ag demand to range from 70 to 260 ktons as Ag paste loading varies.

For In, the future market share of ITO containing technologies is demonstrated to have significant influence on the cumulative demand, which may range from 10 to 300 ktons between 2025 and 2050, as shown in Figure 8(b). Relative to the global resources and reserves estimate of 50 ktons in 2009 [14], the market share of ITO-containing silicon-based PV technologies would need to remain below approximately 15% under high-deployment scenarios and below 30% under low-deployment scenarios to avoid the PV sector alone exhausting current reserve and resource estimate by 2050. This represents an absolute upper bound, as it does not account for indium demand from other industries. As such, thinner ITO layers and zinc oxide-based alternatives [88] are essential for enabling a high future market share for the SHJ, IBC-SHJ, and Pvk-SHJ-tandem technologies.

For solar-grade Si, the cumulative demand between 2025 and 2050 is projected to range from 50 to 160 Mtons depending on wafer thickness, kerf losses, and installed capacity, as shown in Figure 9. Variation in installed capacity alone represents 85% of the maximum demand range, while variation in wafer thickness and kerf losses represent 40% and 20%, respectively. The overlap (>100%) is an indication of parameter interactions. Furthermore, these trends show that demand growth dominates silicon requirements, even more than the anticipated material intensity reductions.

From Figure E-2 in Appendix E, the cumulative demand for Al between 2025 and 2050 is projected to range from 450 to 1 260 Mtons, considering the market share of aluminum module frames and total installed capacity. Based on the maximum range of cumulative Al demand attributable to each variable, variation in installed capacity accounts for 89% of this range, whereas the variation in market share of aluminum module frames accounts for 26%. As such, demand growth remains the primary driver; yet, changes in design choices regarding frame materials could meaningfully influence long-term Al demand. From Figure E-3 in Appendix E, Cu demand over the same period is expected to range from 130 to 400 Mtons, considering inverter and cabling learning rates alongside total installed capacity. Ongoing innovations, such as high-voltage inverters (2 000 V) and alternative cabling materials (aluminum), could improve the learning rates of these components and help reduce future Cu demand [89], [90].

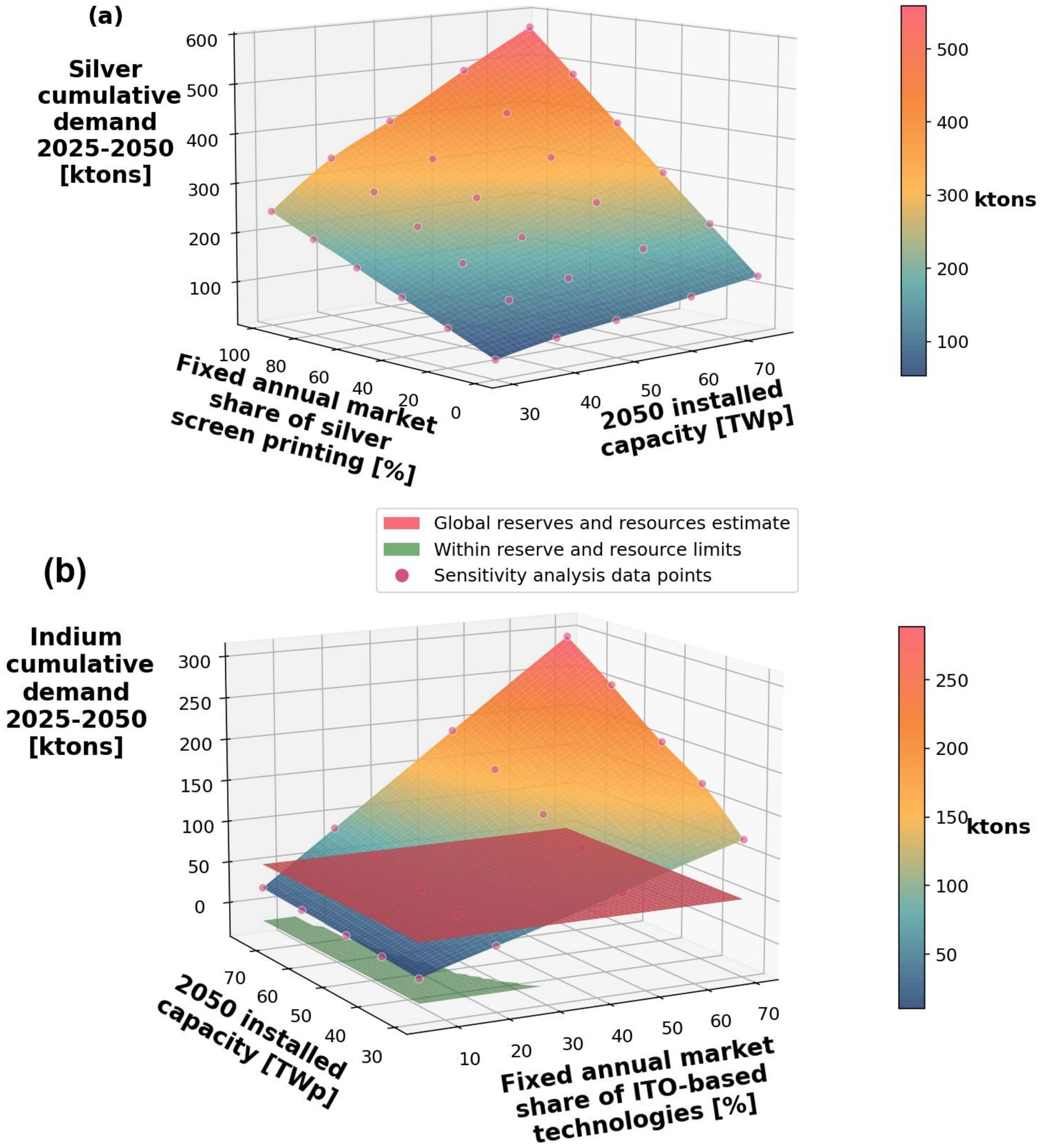

Figure 8: Sensitivity analysis results of cumulative silver and indium demand from the PV sector, 2025-2050 in ktons. (a) X-axis is the 2050 installed capacity for each of the five deployment scenarios, Y-axis is the fixed value assumed for the market share of silver screen printing in cell metallization, remaining share is allocated to copper screen printing and copper plating as described in section 2.2, Z-axis is the cumulative silver demand in ktons. (b) X-axis is the fixed value assumed for the market share of ITO-based technologies (SHJ, IBC-SHJ, & Pvk-Si-tandem), remaining share is allocated TOPCon & IBC-TOPCon as described in section 2.2, Z-axis is the cumulative indium demand in ktons. The reserve and resource estimate is represented by a horizontal plane at 50 ktons, which intersects with the cumulative demand plane, and values less than 50 ktons are projected on the green plane.

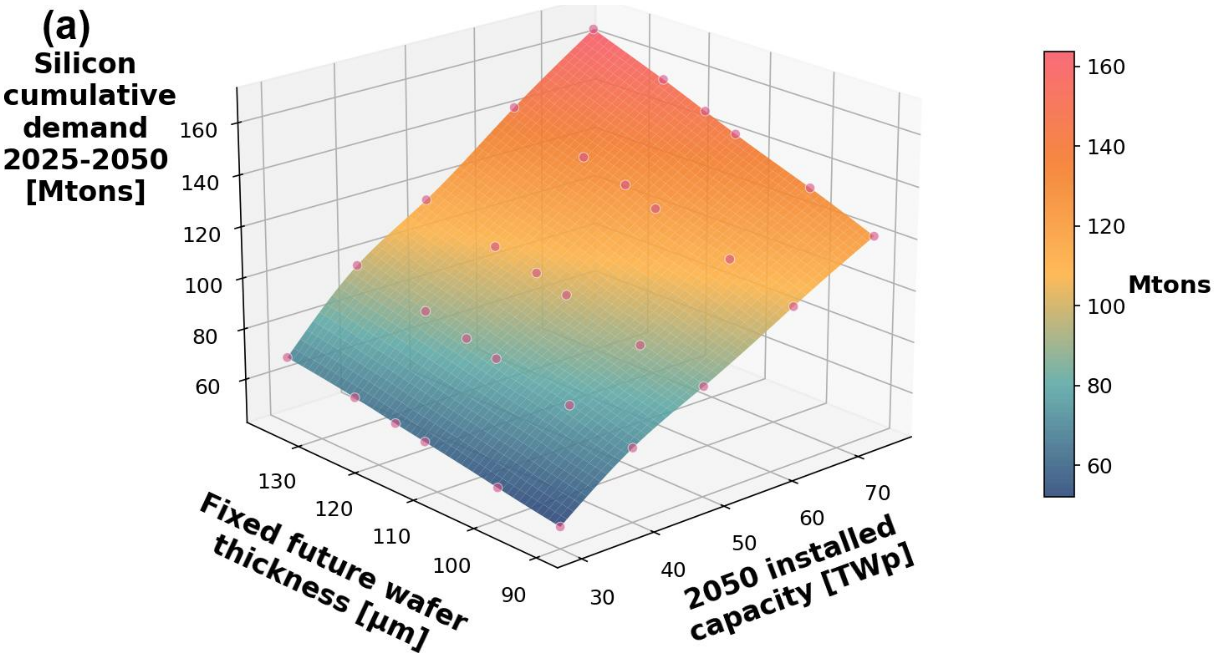

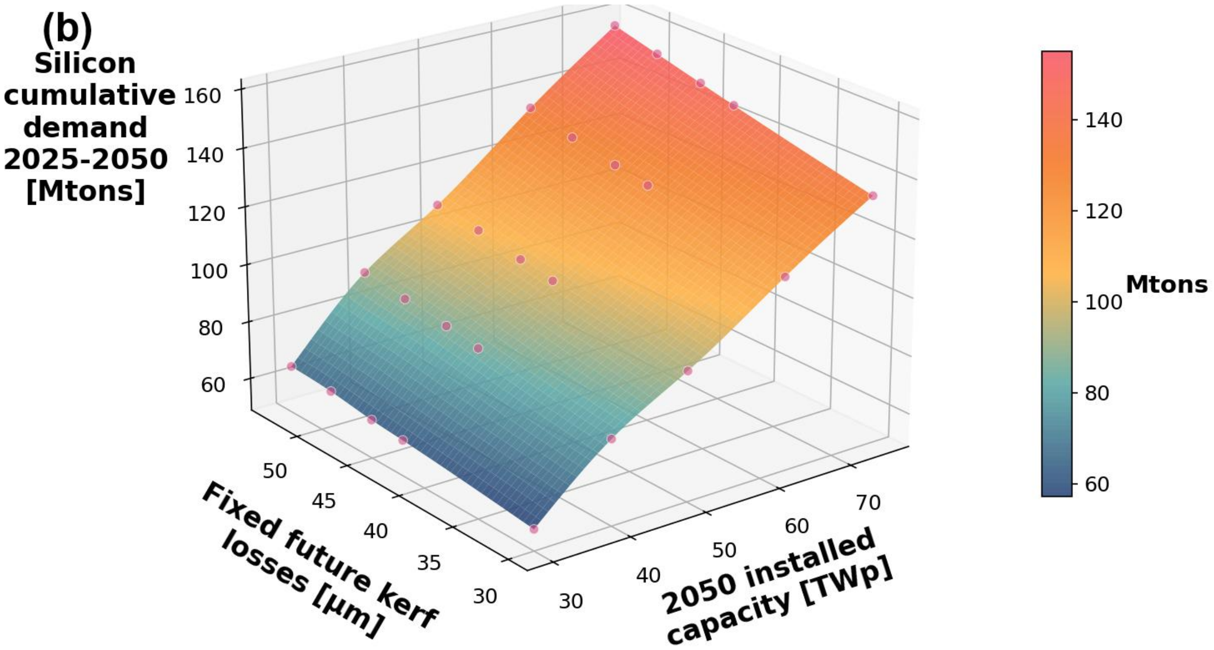

Figure 9: Sensitivity analysis results of cumulative silicon demand from the PV sector, 2025-2050 in Mtons. (a) X-axis is the 2050 installed capacity for each of the five deployment scenarios, Y-axis is the fixed value assumed for the wafer thickness, Z-axis is the cumulative silicon demand in Mtons. (b) X-axis is the 2050 installed capacity for each of the five deployment scenarios, Y-axis is the fixed value assumed for the kerf losses, Z-axis is the cumulative silicon demand in Mtons.

3.3 Resource-use impacts

The results of the four methods for assessing the cumulative resource-use of the global silicon-based PV sector between 2025 and 2050 are summarized in Table 3-1 and Table B-1 in Appendix B. Under the ADP_{UR} method, Au emerges as the largest contributor to ADP_{UR} impacts (56%), entirely driven by the demand for inverters. This disproportionate impact reflects the scarcity weighting embedded in the ADP_{UR} method, an inherent bias acknowledged by the original methodology's authors, who reported that Au alone accounts for 70% of global annual ADP_{UR} impacts [67]. Cu ranks as the second-largest contributor (33%), due to the significant demand in cabling and inverters and given the limited global reserves available relative to annual mine production. Ag ranks as the third-largest contributor (13%), similarly representing a case in which a metal with limited ultimate reserves dominate ADP_{UR} rankings despite its relatively dilute concentration in silicon-based PV systems. These results align with those from the study by Frischknecht and Krebs for mono c-Si residential PV systems [29]. However, the lower contribution from silver in this study is due to anticipated reductions in silver material intensity and substitution by copper-based metallization.

For the low deployment scenario, total ADP_{UR} impacts are estimated at 10 Mt Sb eq., which is approximately 47% lower than the high deployment scenario. Regarding closed-loop recycling, subtracting the total material mass of the cumulative waste stream (2025-2050) from the cumulative demand results in ADP_{UR} impact reductions of 25% and 17% for the low and high deployment scenarios, respectively. These figures represent an upper-bound estimate of the potential benefits of 100% material recovery, without accounting for real-world constraints such as collection rates for EoL PV systems and recovery efficiencies in industrial recycling processes. Notably, In contributes to 97% of the economic resource scarcity impacts using the ADP_{ER} method. This dominance is attributed to the low annual production volumes and limited reserve base assumed for indium in the 2015 reference year used in the characterization factors [67]. For the SOP_{URR} method, Cu and Al together account for about 76% of total impacts, consistent with the study by Vieira et al. [68], which identified them among the top five contributors to global SOP_{URR} impacts. Frischknecht and Krebs [29], however, estimated a higher contribution from gold, which can be attributed to differences in gold intensity assumptions: their estimate implies approximately 2.05 g Au/kWp, derived from a gold intensity of 0.07 mg/kWh AC electricity, an average lifetime yield of 975 kWh/kWp/year, and a 30-year panel lifetime. In contrast, this study applies gold intensities of 0.15 g/kWp for residential inverters and 0.02 g/kWp for utility-scale inverters in 2025, both scaled using an 11% learning curve, which results in considerably lower gold demand and a correspondingly smaller contribution to total SOP_{URR} impacts.

Under the ESSENZ method, In emerges as the largest contributor to total criticality impacts of the PV sector, accounting for an average of 75% across the two deployment scenarios. This high score is driven by several factors: (1) the limited feasibility of new exploration projects, as reflected in the Policy Potential Index for political and societal conditions in producing countries; (2) the small size of global reserves when compared to annual mining production (resulting in rapid depletion under current extraction rates); and (3) the strong geographical concentration of those reserves in a few countries [70]. Sn emerges as the second-largest contributor (9%), which is due to the relatively small volume of global reserves compared to the annual mine production and historic market price fluctuations [70]. Ag has an average contribution of 6% across the two deployment scenarios mainly due to demand growth and the limited contribution of secondary raw materials to silver consumption [70].

Regarding closed-loop recycling, subtracting the total material mass of the cumulative waste stream generated between 2025 and 2050 from the projected cumulative demand results in a reduction in criticality impacts of approximately 12% and 8% for the low and high deployment scenarios, respectively as demonstrated in Table B-1 in Appendix B. Under these conditions, the contribution of In to the overall criticality score increases to an average of 78 % across the two scenarios. This is primarily due to the limited extent to which recycled In can meet the rapidly increasing future demand, despite noticeable reductions in all remaining raw materials. In contrast, the projected reduction in primary demand for Ag results in a 23% average decrease in its contribution to criticality impacts. Furthermore, closed-loop recycling may result in significant reductions in the ADP_{UR} and SOP_{URR} impacts by the PV sector due to the cumulative EoL PV waste stream content of Cu, Al, and Au, as shown in the results in Table B-1.

Table 3-1: Resource-use indicators for the PV sector raw material demands between 2025 and 2050 in Mtons Sb eq., considering the entire cumulative demand (2025-2050)

	Low PV deployment				High PV deployment			
	ADP_{UR}	ESSENZ	ADP_{ER}	SOP_{URR}	ADP_{UR}	ESSENZ	ADP_{ER}	SOP_{URR}
Aluminum	0.00	0.46	0.01	151.16	0.00	0.92	0.02	303.64
Copper	3.10	0.76	0.57	253.83	5.95	1.46	1.10	487.71
Indium	0.01	13.56	67.34	10.51	0.01	30.70	152.42	23.79
Lead	0.01	0.01	0.02	0.69	0.03	0.03	0.04	1.28
Silicon	0.00	0.70	0.00	44.71	0.00	1.41	0.00	90.55
Silver	0.89	1.15	0.84	27.54	1.52	1.96	1.44	47.16
Tin	0.13	1.64	0.13	14.39	0.27	3.33	0.26	29.30
Zinc	0.02	0.07	0.05	1.67	0.03	0.14	0.10	3.18
Gold	5.32	0.13	0.15	25.34	10.09	0.25	0.29	48.11
TOTAL	**9.5**	**18.5**	**69.1**	**529.8**	**17.9**	**40.2**	**155.7**	**1034.7**

4 CONCLUSION

This research made advances to both the characterization of silicon-based PV component material composition, parameterized using ITRPV projections for cell and module-level technical parameters, and to a material flow analysis model to forecast the future demand, in-use stock, end-of-life outflows, and the resulting secondary supply of PV materials as a function of future installed capacity from 2025 to 2050. Then, a sensitivity analysis was also performed to determine the impact of future installation size, technology design parameters, and component-specific learning rates on the future demand of silicon-based PV materials. Finally, resource-use impacts were assessed using the abiotic depletion potential (ADP) ultimate reserves method and the ESSENZ criticality method. The scope of the study included both silicon-based PV modules and BOS components, including inverters, cabling, and mounting structures.

The dMFA model showed an upward trend in materials demand until 2040, which then reverses due to assumptions regarding the lifetime of PV systems and the annual growth rate of new installations. Indium demand has the highest compound annual growth rate (18-24%/y) between 2025 and 2040, due to the anticipated increase in the market share of indium tin oxide-containing silicon-based module technologies. On the contrary, silver has the lowest compound annual growth rate (-4 - 1%/y) during the same period. As a consequence, closed-loop recycling of silver from the waste stream generated between 2025 and 2050 could meet 30-45w% of the cumulative demand during the same period. These figures are strongly influenced by assumptions regarding the anticipated reductions in silver paste loading and the market substitution with copper-based metallization.

A sensitivity analysis confirmed the future growth of installed capacity as the primary driver of cumulative demand for most key silicon-based PV materials. Notable exceptions are silver and indium, where technological parameters play a decisive role. Reductions in silver paste loading and the shift from silver to copper metallization could substantially lower silver demand. For indium, maintaining the market share of indium tin oxide-based technologies under 20% would keep the 2025-2050 cumulative PV sector demand within current global reserves and resources estimate by 2050. However, this represents an absolute upper bound that excludes indium demand from other industries; in practice, a significantly lower market share threshold would be required to ensure adequate supply beyond 2050.

The ADP and ESSENZ methods provide complementary perspectives on resource-use impacts. According to the ADP_{UR} method, which assesses resource depletion impacts based on geological scarcity, copper has the greatest impact due to high PV sector demand and current ultimate reserve depletion rates. Furthermore, despite the very low mass of silver and gold required for PV systems relative to other bulk materials such as aluminum and copper, the cumulative demand from terawatt-scale deployment represents a significant stress on limited global reserves. The ESSENZ method, which assesses potential supply risks associated with primary raw material production, identifies indium as the PV material with the greatest supply risks, accounting for an average of 76% of total criticality impacts across deployment scenarios, driven by limited exploration feasibility, small reserves relative to annual production, and high geographical concentration. Tin (7%) and silver (6%) follow, with tin's criticality driven by limited reserves and price volatility, and silver driven by projected demand growth and limited contribution of secondary material.

5 LIMITATIONS AND FUTURE RESEARCH

Thin film technologies were excluded from the scope of this study on the basis that they currently account for only **2% of the global market**. There are differing views on whether these technologies will maintain their current marginal market share [6], or increase significantly to 10-12% of the total market by 2035 [91]. Future research could include a comprehensive assessment of these potential deployment, as well as the resulting indium, tellurium, and gallium material flows. These materials have **very low global annual mine production** [7], which means that even if thin film technologies maintain a marginal share of the PV market, **terawatt-scale deployment could generate absolute primary and secondary material demands that are significant in a global context and thus warrant further investigation.**

At the cell level, the study does not capture the full range of emerging perovskite technology configurations. Perovskite absorber layers can differ substantially in composition depending on whether they are used in standalone perovskite modules, in tandem with copper indium gallium selenide thin-film devices, or in perovskite-silicon tandems. The dMFA model included only the perovskite-c-Si tandem configuration, which is the most relevant for c-Si PV technologies. At the module level, substitution of aluminum as a module frame material is represented only as a reduction in aluminum demand in the put-on-market stream, without explicitly modeling the corresponding increase in material demand for the alternative frame material (e.g., plastic, steel or composite-based frames). Bismuth in low thermal budget solder alloys for SHJ cells was not included in this analysis due to significant uncertainty surrounding future interconnection configurations (including whether busbarless or alternative designs will become dominant) and the absence of guidance on this topic in the ITRPV roadmap.

A key limitation of the assessment of PV-related indium demand is that the comparison is made against current global resources and reserves estimate without explicitly allocating indium to competing end-use sectors such as displays, electronics, and specialty coatings, which already account for a substantial share of global end-use sector demand. In addition, the analysis does not impose a constraint on preserving indium availability beyond 2050. Accounting for these factors would further tighten the effective indium budget available to the PV sector and strengthen the conclusion that substantial reductions in indium intensity, or a rapid transition to indium-free transparent conductive oxides, are necessary to sustain large-scale future deployment. Because indium is a by-product material and reserve/resource estimates are highly uncertain, these results should be interpreted as highlighting the importance of material-efficiency strategies, substitution options, and competing-sector demand rather than as a definitive forecast. Furthermore, The analysis also does not include potential future indium demand from CIGS thin film PV, which prior indium-demand studies have identified as a potentially important future PV-sector use case [92].

At the system level, material use estimates could be further refined. The present model applies a simplified bill of material for the BOS components and does not distinguish between central and string inverter configurations. In practice, these configurations differ substantially in electronic components, and associated cable layout. Similarly, the modeling of low-voltage AC cabling and DC cable lengths across system designs (utility-scale, residential-scale) assumed fixed per-capacity intensity values, which does not reflect the variation in copper demand with varying site characteristics such as land area and grid proximity. The components excluded from the analysis, including foundations, floating structures, control and communication systems, and battery storage systems, lead to additional material requirements that are not captured in the present results. In particular, these BOS components that were excluded from this analysis may entail further demand for silicon, copper, and aluminum in communication hardware, power electronics, battery current collectors, and internal busbars. In addition, variation in racking and support structure designs (e.g., single-axis tracking versus fixed-tilt systems) can significantly influence material requirements, especially for steel, and is not captured in this analysis. Beyond the materials explicitly assessed, excluded balance-of-system components are also likely to entail additional demand for steel (iron) as well as critical battery and permanent magnet-related materials, including nickel, cobalt, manganese, graphite, and rare earth elements, which are not considered in the scope of this study.

Economic factors such as lower module costs, increased performance, financial incentives, and sales incentives may all contribute to the premature replacement of technically functional PV systems [66]. The lack of representation of these factors in the current analysis may have resulted in underestimations of near- and mid-term waste generation while overestimating the building up of the in-use material stocks. Future work could give attention to economic drivers and replacement behavior to better understand their interactions and effects on in-use stock, inflow, and outflow projections. Collection losses, processing inefficiencies, and material contamination are excluded from the system boundary due to the lack of globally consistent data. A limitation of the OAT sensitivity analysis approach used in this study is that parameters were varied individually and independently. Hence, potential interactions between parameters, as well as with other baseline model assumptions, were not explicitly captured. Future work could address this by applying a global sensitivity analysis framework, which would allow simultaneous variation of multiple parameters and explicitly account for interactions with cell and module efficiency, and future installed capacity.

Future research could examine end-of-life strategies in greater detail, including reuse and remanufacturing, and their impact on raw material demands. To explore an upper bound, the recycling analysis in this study assumes an unrealistic 100% recovery from future waste generation. Extending this to account for realistic collection rates and the material-specific recovery efficiencies of commercial recycling processes and the feasibility of secondary raw material use in new PV manufacturing (i.e., closed-loop recycling) would provide a more complete picture of end-of-life material flows. In addition explicitly modeling the regional distribution of future PV installations would allow estimation of how end-of-life waste streams are distributed across countries and regions, which is important because the scale and timing of recycling and collection needs will differ substantially depending on where capacity is installed. Furthermore, detailed modeling of emerging trends in module and BOS components could improve demand estimates for aluminum and copper. Relevant developments include the transition to higher-voltage and higher-efficiency string and central inverters, silicon carbide-based power electronics, and multi-terminal (including four-terminal) module designs.

REFERENCES

[1] IEA, “Net Zero Roadmap: A Global Pathway to Keep the 1.5 °C Goal in Reach,” Paris, 2023. Accessed: Apr. 10, 2026. [Online]. Available: https://www.iea.org/reports/net-zero-roadmap-a-global-pathway-to-keep-the-15-c-goal-in-reach

[2] IDTechEx, “Flexible Photovoltaics Market 2025-2035: Technologies, Players, and Trends.” Accessed: Apr. 10, 2026. [Online]. Available: https://www.idtechex.com/en/research-report/flexible-photovoltaics-market-2025-2035-technologies-players-and-trends/1081

[3] Tongwei CO. LTD., “What is the advantage of thin film solar panel.” Accessed: Apr. 10, 2026. [Online]. Available: https://en.tongwei.cn/blog/489.html

[4] A. Bett *et al.*, “Photovoltaics Report, updated,” May 2025. Accessed: Aug. 15, 2025. [Online]. Available: https://www.ise.fraunhofer.de/content/dam/ise/de/documents/publications/studies/Photovoltaics-Report.pdf

[5] HCSS, “HCSS Critical Raw Materials Dashboard.” Accessed: Apr. 16, 2025. [Online]. Available: https://hcss.nl/critical-minerals/

[6] N. Taylor *et al.*, “Deep dive on critical raw materials for solar photovoltaics in the EU,” Publications Office of the European Union, Luxembourg (Luxembourg), 2025. doi: 10.2760/0883326 (online),10.2760/9053398 (print).

[7] U.S. Geological Survey, “Mineral commodity summaries 2025 (ver. 1.2, March 2025),” Virginia, 2025. doi: 10.3133/MCS2025.

[8] S. Flowers, G. Thompson, N. Biggs, C. Cooper, and P. Schmitz, “Can copper supply keep up with surging demand? ,” Wood Mackenzie. Accessed: Apr. 16, 2026. [Online]. Available: https://www.woodmac.com/blogs/the-edge/can-copper-supply-keep-up-with-surging-demand/

[9] P. Guj and R. Schodde, “Will future copper resources and supply be adequate to meet the net zero emission goal?,” *Geosystems and Geoenvironment*, vol. 4, no. 1, p. 100320, Feb. 2025, doi: 10.1016/J.GEOGEO.2024.100320.

[10] SunSirs, “Global Polysilicon Demand Projected at 1.02–1.18 Million Metric Tons by 2026.” Accessed: Apr. 16, 2026. [Online]. Available: https://www.sunsirs.com/commodity-news/petail-30003.html

[11] IEA, “Energy Technology Perspectives 2026,” Paris, 2026. Accessed: Apr. 16, 2026. [Online]. Available: https://www.iea.org/reports/energy-technology-perspectives-2026

[12] C. Ramírez-Márquez, “Solar-Grade Silicon in the Energy Transition: A Strategic Commodity for the Global Photovoltaic Market,” *Commodities 2025, Vol. 4,* vol. 4, no. 3, p. 18, Aug. 2025, doi: 10.3390/COMMODITIES4030018.

[13] M. Fischer, M. Woodhouse, T. Brammer, and P. Baliozian, “International Technology Roadmap for Photovoltaics (ITRPV)- 2024 Results,” 2025. Accessed: Jun. 16, 2025. [Online]. Available: https://www.vdma.org/international-technology-roadmap-photovoltaic

[14] M. Lokanc, R. Eggert, and M. Redlinger, “The Availability of Indium: The Present, Medium Term, and Long Term,” 2015. Accessed: Jul. 09, 2025. [Online]. Available: https://docs.nrel.gov/docs/fy16osti/62409.pdf

[15] J. Green, “ITO vs. FTO Films as Transparent Conductive Oxides (TCOs),” Stanford advanced materials. Accessed: Oct. 15, 2025. [Online]. Available: https://www.sputtertargets.net/blog/ito-vs-fto-films-as-transparent-conductive-oxides-tcos.html

[16] A. T. Vai, N. Rashidi, Y. Fang, V. L. Kuznetsov, and P. P. Edwards, “Contrasting the grain boundary-affected performance of zinc and indium oxide transparent conductors,” *Journal of Physics: Condensed Matter*, vol. 28, no. 22, p. 224003, Mar. 2016, doi: 10.1088/0953-8984/28/22/224003.

[17] K. Wambach, C. Libby, and S. Shaw, “Advances in Photovoltaic Module Recycling: Literature Review and Update to Empirical Life Cycle Inventory Data and Patent Review,” 2024. Accessed: Apr. 16, 2026. [Online]. Available: https://iea-pvps.org/wp-content/uploads/2024/06/IEA-PVPS-T12-28-2024-Report-PV-Recycling-LCI_EPRI.pdf

[18] J. P. Casey, “WoodMac: Policies and production cuts to drive up module prices,” PV Tech. Accessed: May 01, 2026. [Online]. Available: https://www.pv-tech.org/chinese-government-policies-production-cuts-drive-up-module-prices-wood-mackenzie/

[19] E. Graham and N. Fulghum, “Solar power continues to surge in 2024,” Ember. Accessed: May 01, 2026. [Online]. Available: https://ember-energy.org/latest-insights/solar-power-continues-to-surge-in-2024/

[20] European Parliament and Council, “Regulation (EU) 2024/1252 on establishing a framework for ensuring a secure and sustainable supply of critical raw materials,” 2024, *EUR-Lex*. Accessed: May 07, 2025. [Online]. Available: https://eur-lex.europa.eu/legal-content/EN/TXT/?uri=CELEX%3A02024R1252-20240503

[21] United States. Congress. House, *Inflation Reduction Act of 2022*. 2022.

[22] MINISTRY OF NEW AND RENEWABLE ENERGY-Government of India, “Production Linked Incentive (PLI) Scheme: National Programme on High Efficiency Solar PV Modules.” Accessed: May 01, 2026. [Online]. Available: https://mnre.gov.in/en/production-linked-incentive-pli/

[23] IRENA and CPI, “Global landscape of energy transition finance 2025,” Abu Dhabi, 2025. Accessed: May 01, 2026. [Online]. Available: https://www.irena.org/-/media/Files/IRENA/Agency/Publication/2025/Nov/IRENA_CPI_FIN_Global_landscape_energy_transition_finance_2025.pdf

[24] IRENA, “World Energy Transitions Outlook 2023: 1.5°C Pathway,” Abu Dhabi, 2023. Accessed: Apr. 16, 2025. [Online]. Available: https://www.irena.org/Publications/2023/Jun/World-Energy-Transitions-Outlook-2023

[25] IEA, “World Energy Outlook 2024,” Paris, 2024. Accessed: Apr. 16, 2025. [Online]. Available: https://www.iea.org/reports/world-energy-outlook-2024

[26] D. Bogdanov *et al.*, “Low-cost renewable electricity as the key driver of the global energy transition towards sustainability,” *Energy*, vol. 227, p. 120467, Jul. 2021, doi: 10.1016/J.ENERGY.2021.120467.

[27] N. M. Haegel *et al.*, “Terawatt-scale photovoltaics: Transform global energy Improving costs and scale reflect looming opportunities,” *Science (1979).*, vol. 364, no. 6443, pp. 836–838, May 2019, doi: 10.1126/SCIENCE.AAW1845/SUPPL_FILE/AAW1845-HAEGEL-SM.PDF.

[28] S. . Bobba, S. . Carrara, J. . Huisman, F. . Mathieux, and C. . Pavel, *Critical raw materials for strategic technologies and sectors in the EU : a foresight study*. Publications Office of the European Union, 2020. doi: 10.2873/58081.

[29] R. Frischknecht and L. Krebs, “Resource Use Footprints of Residential PV Systems,” 2022. Accessed: Aug. 15, 2025. [Online]. Available: https://iea-pvps.org/key-topics/mineral-resource-use-footprints-of-residential-pv-systems/

[30] Y. Zhang, M. Kim, L. Wang, P. Verlinden, and B. Hallam, “Design considerations for multi-terawatt scale manufacturing of existing and future photovoltaic technologies: challenges and opportunities related to silver, indium and bismuth consumption,” *Energy Environ. Sci.*, vol. 14, no. 11, pp. 5587–5610, Nov. 2021, doi: 10.1039/D1EE01814K.

[31] L. Wang *et al.*, “Sustainability evaluations on material consumption for terawatt-scale manufacturing of silicon-based tandem solar cells,” *Progress in Photovoltaics: Research and Applications*, vol. 31, no. 12, pp. 1442–1454, Dec. 2023, doi: 10.1002/PIP.3687;WGROUP:STRING:PUBLICATION.

[32] B. Hallam *et al.*, “The silver learning curve for photovoltaics and projected silver demand for net-zero emissions by 2050,” *Progress in Photovoltaics: Research and Applications*, vol. 31, no. 6, pp. 598–606, Jun. 2023, doi: 10.1002/PIP.3661.

[33] M. I. Yacouba *et al.*, “Achieving High Efficiencies for Silicon Heterojunction Solar Cells Using Silver-Free Metallization,” *Progress in Photovoltaics: Research and Applications*, vol. 33, no. 11, pp. 1223–1235, Nov. 2025, doi: 10.1002/PIP.70016;WGROUP:STRING:PUBLICATION.

[34] Y. Zhang *et al.*, “Silver-lean screen-printing metallisation for industrial TOPCon solar cells: Enabling an 80 % reduction in silver consumption,” *Solar Energy Materials and Solar Cells*, vol. 288, p. 113654, Aug. 2025, doi: 10.1016/J.SOLMAT.2025.113654.

[35] K. Guzik, A. Burkowicz, and J. Szlugaj, “The EU’s demand for selected critical raw materials used in the photovoltaic industry,” *Gospodarka Surowcami Mineralnymi - Mineral Resources Management*, vol. 38, no. 2, pp. 31–59, 2022, doi: 10.24425/GSM.2022.141666.

[36] B. Hallam, M. Kim, R. Underwood, S. Drury, L. Wang, and P. Dias, “A Polysilicon Learning Curve and the Material Requirements for Broad Electrification with Photovoltaics by 2050,” *Solar RRL*, vol. 6, no. 10, p. 2200458, Oct. 2022, doi: 10.1002/SOLR.202200458;JOURNAL:JOURNAL:2367198X;WGROUP:STRING:PUBLICATION.

[37] C. Xu, O. Isabella, and M. R. Vogt, “Future material demand for global silicon-based PV modules under net-zero emissions target until 2050,” *Resour. Conserv. Recycl.*, vol. 210, p. 107824, Nov. 2024, doi: 10.1016/J.RESCONREC.2024.107824.

[38] European Commission, “Reuse of Si-kerf-loss for producing mc-Si ingots.” Accessed: Dec. 18, 2025. [Online]. Available: https://innovation-radar.ec.europa.eu/innovation/22004

[39] ICARUS, “Process development and industrial scale demonstrator for silicon kerf into powder applications.” Accessed: Dec. 18, 2025. [Online]. Available: https://www.icarus.eu.com/process-development-and-industrial-scale-demonstrator-for-silicon-kerf-into-powder-applications/

[40] J. Li *et al.*, “Progress in recovery and recycling of kerf loss silicon waste in photovoltaic industry,” *Sep. Purif. Technol.*, vol. 254, p. 117581, Jan. 2021, doi: 10.1016/J.SEPPUR.2020.117581.

[41] C. Li, F. Dong, and V. Nian, “Global photovoltaic waste under ratcheting climate ambition: Spatio-temporal distribution and future pathways,” *Resour. Conserv. Recycl.*, vol. 221, p. 108388, Jul. 2025, doi: 10.1016/J.RESCONREC.2025.108388.

[42] E. Kastanaki, “Dynamic assessment of photovoltaic waste streams in the EU-27 countries under the circular economy principles of ‘Reduce, Reuse and Recycle,’” *Resour. Conserv. Recycl.*, vol. 214, p. 108033, Mar. 2025, doi: 10.1016/J.RESCONREC.2024.108033.

[43] B. Liu, H. Wang, X. Liang, Y. Wang, and Z. Feng, "Recycling to alleviate the gap between supply and demand of raw materials in China's photovoltaic industry," *Resour. Conserv. Recycl.*, vol. 201, p. 107324, Feb. 2024, doi: 10.1016/J.RESCONREC.2023.107324.

[44] SolarPower Europe, "Cumulative installed solar PV capacity worldwide from 2000 to 2024 (in megawatts) [Graph]," Statista. Accessed: Jul. 16, 2025. [Online]. Available: https://www.statista.com/statistics/280220/global-cumulative-installed-solar-pv-capacity/

[45] D. Intal and A. U. Ebong, "Thin-film solar photovoltaics: Trends and future directions," *Renewable and Sustainable Energy Reviews*, vol. 226, p. 116464, Jan. 2026, doi: 10.1016/J.RSER.2025.116464.

[46] H. Lin *et al.*, "Silicon heterojunction solar cells with up to 26.81% efficiency achieved by electrically optimized nanocrystalline-silicon hole contact layers," *Nat. Energy*, vol. 8, no. 8, pp. 789–799, May 2023, doi: 10.1038/s41560-023-01255-2.

[47] Z. Yang, "Sunket HJT Solar Panel Advantages & Practical Application Analysis," SUNKET. Accessed: Jul. 16, 2025. [Online]. Available: https://sunketpower.com/sunket-hjt-solar-panel-advantages-practical-application-analysis/

[48] M. H. Futscher and B. Ehrler, "Efficiency Limit of Perovskite/Si Tandem Solar Cells," *ACS Energy Lett.*, vol. 1, no. 4, pp. 863–868, Oct. 2016, doi: 10.1021/ACSENERGYLETT.6B00405/ASSET/IMAGES/LARGE/NZ-2016-004056_0005.JPEG.

[49] C. Xu, O. Isabella, and M. R. Vogt, "Projected technical innovations could solve silver demand crisis in the terawatt-scale photovoltaics era," *submitted for publication*, 2025.

[50] E. Bellini, "Fraunhofer ISE developing heterojunction solar cells with silver consumption of less than 2 mg per W," pv magazine. Accessed: Jul. 17, 2025. [Online]. Available: https://www.pv-magazine.com/2025/04/17/fraunhofer-ise-developing-heterojunction-solar-cells-with-silver-consumption-of-less-than-2-mg-per-w/

[51] N. Chen, D. Rudolph, C. Peter, H. Chu, T. Buck, and V. D. Mihailetchi, "Screen printed copper paste for metallization of IBC solar cells," in *AIP Conf. Proc.*, 2023, pp. 2826, 090001. doi: 10.1063/5.0140623.

[52] B. L. Smith, A. Sekar, H. Mirletz, G. Heath, and R. Margolis, "An Updated Life Cycle Assessment of Utility-Scale Solar Photovoltaic Systems Installed in the United States," Golden, CO, Mar. 2024. Accessed: Jul. 18, 2025. [Online]. Available: https://www.nrel.gov/docs/fy24osti/87372.pdf

[53] MakeItFrom.com, "6005A-T6 Aluminum." Accessed: Apr. 20, 2026. [Online]. Available: https://www.makeitfrom.com/material-properties/6005A-T6-Aluminum

[54] IEA, "Solar PV power capacity in the Net Zero Scenario, 2015-2030," IEA, Paris. Accessed: Jul. 17, 2025. [Online]. Available: https://www.iea.org/data-and-statistics/charts/solar-pv-power-capacity-in-the-net-zero-scenario-2015-2030

[55] D. Olson and B. E. Bakken, "Utility-scale solar PV: From big to biggest," DNV. Accessed: Jul. 17, 2025. [Online]. Available: https://www.dnv.com/feature/utility-scale-solar/

[56] M. Götz *et al.*, *Life Cycle Inventories of Photovoltaic Systems*. International Energy Agency (IEA) PVPS Task 12, Report T12- 33:2026, 2026.

[57] M. Aliang, "The Future Material Demand for Inverters and Cabling used in Photovoltaic (PV) Systems," Master Thesis, TU Delft, 2024. Accessed: Jul. 17, 2025. [Online]. Available: https://resolver.tudelft.nl/uuid:d7e82288-45d1-492a-ab74-1c288a7981ff

[58] A. M. Elshurafa, S. R. Albardi, S. Bigerna, and C. A. Bollino, "Estimating the learning curve of solar PV balance–of–system for over 20 countries: Implications and policy recommendations," *J. Clean. Prod.*, vol. 196, pp. 122–134, Sep. 2018, doi: 10.1016/j.jclepro.2018.06.016.

[59] P. Xie, "Future material demand and associated environmental impacts for aluminum used in global PV systems," TU Delft, 2024. Accessed: Jul. 17, 2025. [Online]. Available: https://resolver.tudelft.nl/uuid:e22ad847-5241-4e2a-a7ce-d4279145321f

[60] A. Müller, L. Friedrich, C. Reichel, S. Herceg, M. Mittag, and D. H. Neuhaus, "A comparative life cycle assessment of silicon PV modules: Impact of module design, manufacturing location and inventory," *Solar Energy Materials and Solar Cells*, vol. 230, p. 111277, Sep. 2021, doi: 10.1016/J.SOLMAT.2021.111277.

[61] M. Roffeis *et al.*, "New insights into the environmental performance of perovskite-on-silicon tandem solar cells – a life cycle assessment of industrially manufactured modules," *Sustain. Energy Fuels*, vol. 6, no. 12, pp. 2924–2940, Jun. 2022, doi: 10.1039/D2SE00096B.

[62] PV-LAB - EPFL, "Silicon-based heterojunction solar cells," EPFL. Accessed: Jul. 18, 2025. [Online]. Available: https://www.epfl.ch/labs/pvlab/research/heterojunction_solar_cells/

[63] I. Celik, Z. Song, A. J. Cimaroli, Y. Yan, M. J. Heben, and D. Apul, "Life Cycle Assessment (LCA) of perovskite PV cells projected from lab to fab," *Solar Energy Materials and Solar Cells*, vol. 156, pp. 157–169, Nov. 2016, doi: 10.1016/J.SOLMAT.2016.04.037.

[64] TU Delft, "Doping-Part 1." Accessed: Apr. 20, 2026. [Online]. Available: https://delftxdownloads.tudelft.nl/PV2x/2.3.2.1/PV2x_2017_2.3.2.1_Doping_Part_1-transcript.pdf

[65] S. Pauliuk and N. Heeren, "ODYM—An open software framework for studying dynamic material systems: Principles, implementation, and data structures," *J. Ind. Ecol.*, vol. 24, no. 3, pp. 446–458, Jun. 2020, doi: 10.1111/JIEC.12952;REQUESTEDJOURNAL:JOURNAL:15309290;WGROUP:STRING:PUBLICATION.

[66] V. Tan, P. R. Dias, N. Chang, and R. Deng, "Estimating the Lifetime of Solar Photovoltaic Modules in Australia," *Sustainability 2022, Vol. 14, Page 5336*, vol. 14, no. 9, p. 5336, Apr. 2022, doi: 10.3390/SU14095336.

[67] L. van Oers, J. B. Guinée, and R. Heijungs, "Abiotic resource depletion potentials (ADPs) for elements revisited—updating ultimate reserve estimates and introducing time series for production data," *International Journal of Life Cycle Assessment*, vol. 25, no. 2, pp. 294–308, Feb. 2020, doi: 10.1007/S11367-019-01683-X/FIGURES/5.

[68] M. D. M. Vieira, T. C. Ponsioen, M. J. Goedkoop, and M. A. J. Huijbregts, "Surplus Ore Potential as a Scarcity Indicator for Resource Extraction," *J. Ind. Ecol.*, vol. 21, no. 2, pp. 381–390, Apr. 2017, doi: 10.1111/JIEC.12444;REQUESTEDJOURNAL:JOURNAL:15309290;WGROUP:STRING:PUBLICATION.

[69] V. Bach *et al.*, "Integrated method to assess resource efficiency – ESSENZ," *J. Clean. Prod.*, vol. 137, pp. 118–130, Nov. 2016, doi: 10.1016/J.JCLEPRO.2016.07.077.

[70] V. Bach, S. Marinova, and M. Finkbeiner, "Updated data and characterization factors of the criticality assessment for the integrated method to assess resource efficiency (ESSENZ and ESSENZ+)," *Discover Sustainability*, vol. 5, no. 1, pp. 1–5, Dec. 2024, doi: 10.1007/S43621-024-00513-X/TABLES/1.

[71] D. Ioannidou, N. Heeren, G. Sonnemann, and G. Habert, “The future in and of criticality assessments,” *J. Ind. Ecol.*, vol. 23, no. 4, pp. 751–766, Aug. 2019, doi: 10.1111/JIEC.12834.

[72] M. Tao *et al.*, “Major challenges and opportunities in silicon solar module recycling,” *Progress in Photovoltaics: Research and Applications*, vol. 28, no. 10, pp. 1077–1088, Oct. 2020, doi: 10.1002/PIP.3316;WGROUP:STRING:PUBLICATION.

[73] R.-T. Zhan *et al.*, “Recent Advances in Recycling of Copper-Based Waste Materials: A Critical Review,” *cMat*, vol. 2, no. 2, p. e70005, Jun. 2025, doi: 10.1002/CMT2.70005.

[74] J. M. Cullen and J. M. Allwood, “Mapping the global flow of aluminum: From liquid aluminum to end-use goods,” *Environ. Sci. Technol.*, vol. 47, no. 7, pp. 3057–3064, Apr. 2013, doi: 10.1021/ES304256S/SUPPL_FILE/ES304256S_SI_001.PDF.

[75] D. Raabe, C. C. Tasan, and E. A. Olivetti, “Strategies for improving the sustainability of structural metals,” *Nature 2019 575:7781*, vol. 575, no. 7781, pp. 64–74, Nov. 2019, doi: 10.1038/s41586-019-1702-5.

[76] G. A. Heath *et al.*, “Research and development priorities for silicon photovoltaic module recycling to support a circular economy,” *Nature Energy 2020 5:7*, vol. 5, no. 7, pp. 502–510, Jul. 2020, doi: 10.1038/s41560-020-0645-2.

[77] I. M. Peters, J. Hauch, and C. Brabec, “Cradle-to-cradle recycling in terawatt photovoltaics: A vision of perpetual utility,” *Joule*, vol. 8, no. 4, pp. 899–912, Apr. 2024, doi: 10.1016/J.JOULE.2024.01.025.

[78] L. Xu *et al.*, “Waste ITO target recycling for efficient indium recovery through a closed-loop process,” *J. Environ. Chem. Eng.*, vol. 12, no. 2, p. 112136, Apr. 2024, doi: 10.1016/J.JECE.2024.112136.

[79] W. Xu, X. Chen, D. Liu, W. Jiang, and B. Yang, “Systematic thermodynamic and experimental studies for recovering indium and tin from indium tin oxide waste target with hydrogen,” *J. Clean. Prod.*, vol. 429, p. 139328, Dec. 2023, doi: 10.1016/J.JCLEPRO.2023.139328.

[80] Q. An, J. Li, and H. Fang, “Copper target erosion during unbalanced magnetron sputtering under different electromagnetic fields,” *Surf. Coat. Technol.*, vol. 477, p. 130360, Feb. 2024, doi: 10.1016/J.SURFCOAT.2023.130360.

[81] AEM Deposition, “Development Trend of ITO Sputtering Target.” Accessed: Dec. 29, 2025. [Online]. Available: https://www.aemdeposition.com/blog/development-trend-of-ito-sputtering-target.html

[82] M. Scherer, T. Fritz, M. Klosch, and J. Pistner, “High target utilization for ITO of more than 60% with a new planar magnetron cathode,” in *Society of Vacuum Coaters 49 th Annual Technical Conference Proceedings*, 2006.

[83] D. S. Prasad, P. P. Srinivasa Kumar, B. Sanjana, D. Sai Kiran, A. Kamaraj, and R. Ratheesh, “A novel approach for the efficient recovery of lead from End-of-Life Silicon Photovoltaic modules,” *Solar Energy Materials and Solar Cells*, vol. 266, p. 112672, Mar. 2024, doi: 10.1016/J.SOLMAT.2023.112672.

[84] Q. Xiong, Z. Yuan, Y. Zhang, Z. Chen, K. Wei, and W. Ma, “A new approach for separating copper, tin, and lead from photovoltaic ribbon wastes,” *Solar Energy*, vol. 299, p. 113810, Oct. 2025, doi: 10.1016/J.SOLENER.2025.113810.

[85] pv magazine, “PV module recycling gains momentum as waste volumes surge globally.” Accessed: Apr. 22, 2026. [Online]. Available: https://www.pv-magazine.com/2025/10/17/pv-module-recycling-gains-momentum-as-waste-volumes-surge-globally/

[86] X. Zhu, Y. Li, Y. Zhang, Y. Sun, W. Xu, and L. Bai, “Emission reduction optimization of recycling pathways for retired photovoltaic modules in China: A coupled model of life cycle assessment and evolutionary game theory,” *J. Clean. Prod.*, vol. 549, p. 147786, Mar. 2026, doi: 10.1016/J.JCLEPRO.2026.147786.

[87] F. Ardente, C. E. L. Latunussa, and G. A. Blengini, “Resource efficient recovery of critical and precious metals from waste silicon PV panel recycling,” *Waste Management*, vol. 91, pp. 156–167, May 2019, doi: 10.1016/J.WASMAN.2019.04.059.

[88] G. T. Chavan *et al.*, “A Brief Review of Transparent Conducting Oxides (TCO): The Influence of Different Deposition Techniques on the Efficiency of Solar Cells,” *Nanomaterials 2023, Vol. 13, Page 1226*, vol. 13, no. 7, p. 1226, Mar. 2023, doi: 10.3390/NANO13071226.

[89] S&P Global Commodity Insights, “Top 5 global inverter trends to watch in 2025,” pv magazine. Accessed: Aug. 13, 2025. [Online]. Available: https://www.pv-magazine.com/2025/01/29/top-5-global-inverter-trends-to-watch-in-2025/

[90] SUNKEAN, “Analysis of the Trend of Aluminum Solar Cables Replacing Copper Solar Cables,” SUNKEAN. Accessed: Aug. 13, 2025. [Online]. Available: https://www.sunkean.com/blog/Analysis-of-the-Trend-of-Aluminum-Solar-Cables-Replacing-Copper-Solar-Cables_b6288

[91] GlobeNewswire, “Thin Film Photovoltaics Global Market Report 2025-2035: Thin Film Photovoltaics to Capture 10-12% of Global Solar Market by 2035.” Accessed: Nov. 17, 2025. [Online]. Available: https://www.globenewswire.com/news-release/2025/03/17/3043488/0/en/Thin-Film-Photovoltaics-Global-Market-Report-2025-2035-Thin-Film-Photovoltaics-to-Capture-10-12-of-Global-Solar-Market-by-2035.html

[92] J. Lin, X. Li, M. Wang, L. Liu, and T. Dai, “How Can China’s Indium Resources Have a Sustainable Future? Research Based on the Industry Chain Perspective,” *Sustainability 2021, Vol. 13, Page 12042*, vol. 13, no. 21, p. 12042, Oct. 2021, doi: 10.3390/SU132112042.

A. APPENDIX: STARTING PV TECHNOLOGY MATERIAL COMPOSITION *[2025]*

Table A- 1: Material breakdown in kilograms for a 1 kWp monofacial PV system, BOS components are modeled based on the market share of residential and utility installations assumed

	PERC	TOPCon	SHJ	IBC-TOPCon	IBC-SHJ	Pvk-Si-tandem
Cell, wafer, silicon	1.960	1.857	1.661	1.938	1.938	1.440
Cell, Al_2O_3, aluminum	9.7E-05					
Cell, SiN_x, silicon	6.6E-04					
Cell, SiO_2, silicon		1.5E-05		1.5E-05		
Cell, doped poly-Si, silicon		1.4E-03		1.4E-03		
Cell, ITO, indium			3.0E-03		3.0E-03	2.6E-03
Cell, ITO, tin			7.3E-04		7.2E-04	6.3E-04
Cell, amorphous silicon, silicon			3.0E-04		3.0E-04	2.6E-04
Cell, IZO, indium						1.7E-03
Cell, IZO, zinc						2.0E-04
Cell, SnO2, tin						2.1E-04
Cell, perovskite, lead						1.9E-03
Cell, rear contact, aluminum	0.108	0.102		0.100		
Cell, metallization, silver	8.3E-03	0.011	0.013	9.8E-03	9.8E-03	0.013
Cell, metallization, copper	2.3E-03	2.1E-03	2.1E-03	2.1E-03	2.1E-03	1.8E-03
Module, solder alloy, lead	0.043	0.040	0.040	0.040	0.040	0.035
Module, solder alloy, tin	0.048	0.046	0.045	0.045	0.045	0.039
Module, interconnect/cell, copper	0.686	0.650	0.644	0.638	0.638	0.558
Module, plastics	5.968	5.653	5.602	5.546	5.546	4.856
Module, front glass	32.099	30.402	30.127	29.825	29.825	26.116

	PERC	TOPCon	SHJ	IBC-TOPCon	IBC-SHJ	Pvk-Si-tandem
Module, frame, aluminum	6.116	5.793	5.740	5.683	5.683	4.976
Residential inverter, copper	0.100					
Residential inverter, steel	0.301					
Residential inverter, aluminum	0.112					
Residential inverter, zinc	0.040					
Residential inverter, lead	1.1E-03					
Residential inverter, gold	2.4E-05					
Residential inverter, tin	2.1E-03					
Utility inverter, copper	0.156					
Utility inverter, steel	0.310					
Utility inverter, aluminum	0.350					
Utility inverter, zinc	0.024					
Utility inverter, lead	6.9E-04					
Utility inverter, gold	1.8E-05					
Utility inverter, tin	1.6E-03					
Residential installation, cable copper	1.311					
Utility installation, cable copper	2.938					
Mounting structure, open-ground, aluminum	5.505					
Mounting structure, flat-roof, aluminum	3.320					
Mounting structure, slanted-roof, aluminum	4.299					
TOTAL	**65.811**	**63.329**	**62.650**	**62.600**	**62.502**	**56.814**

Table A- 2: Material breakdown in kilograms for a 1 kWp bifacial PV system, BOS components are modeled based on the market share of residential and utility installations assumed

	PERC	TOPCon	SHJ	IBC-TOPCon	IBC-SHJ	Pvk-Si-tandem
Cell, wafer, silicon	1.916	1.817	1.626	1.898	1.898	1.413
Cell, Al_2O_3, aluminum	9.5E-05					
Cell, SiN_x, silicon	6.5E-04					
Cell, SiO_2, silicon		1.5E-05		1.5E-05		
Cell, doped poly-Si, silicon		1.4E-03		1.4E-03		
Cell, ITO, indium			2.9E-03		2.9E-03	2.5E-03
Cell, ITO, tin			7.1E-04		7.0E-04	6.2E-04
Cell, amorphous silicon, silicon			3.0E-04		2.9E-04	2.6E-04
Cell, IZO, indium						1.7E-03
Cell, IZO, zinc						2.0E-04
Cell, SnO2, tin						2.0E-04
Cell, perovskite, lead						1.9E-03
Cell, rear contact, aluminum	0.028	0.026		0.026		
Cell, metallization, silver	8.1E-03	0.011	0.013	9.6E-03	9.6E-03	0.013
Cell, metallization, copper	2.2E-03	2.1E-03	2.1E-03	2.1E-03	2.1E-03	1.8E-03
Module, solder alloy, lead	0.042	0.039	0.039	0.039	0.039	0.034
Module, solder alloy, tin	0.047	0.045	0.044	0.044	0.044	0.039
Module, interconnect/cell, copper	0.636	0.636	0.631	0.624	0.624	0.548
Module, plastics	5.050	5.050	5.006	4.957	4.957	4.352
Module, front glass	31.372	29.748	29.485	29.196	29.196	25.633
Module, back glass	27.503	26.080	25.849	25.596	25.596	22.472
Module, frame, aluminum	5.978	5.668	5.618	5.563	5.563	4.884

	PERC	TOPCon	SHJ	IBC-TOPCon	IBC-SHJ	Pvk-Si-tandem
Residential inverter, copper	0.100					
Residential inverter, steel	0.301					
Residential inverter, aluminum	0.112					
Residential inverter, zinc	0.040					
Residential inverter, lead	1.1E-03					
Residential inverter, gold	2.4E-05					
Residential inverter, tin	2.1E-03					
Utility inverter, copper	0.156					
Utility inverter, steel	0.310					
Utility inverter, aluminum	0.350					
Utility inverter, zinc	0.024					
Utility inverter, lead	6.9E-04					
Utility inverter, gold	1.8E-05					
Utility inverter, tin	1.6E-03					
Residential installation, cable copper	1.311					
Utility installation, cable copper	2.938					
Mounting structure, open-ground, aluminum	5.505					
Mounting structure, flat-roof, aluminum	3.320					
Mounting structure, slanted-roof, aluminum	4.299					
TOTAL	**91.355**	**87.895**	**87.089**	**86.728**	**86.704**	**78.169**

B. APPENDIX: ADDITIONAL RESOURCE-USE IMPACT RESULTS

Table B-1: Resource-use indicators for the PV sector raw material demands between 2025 and 2050 in Mtons Sb eq., considering the net primary demand (2025-2050) [subtracting material content in the cumulative outflow PV waste stream (2025-2050)]

	Low PV deployment				High PV deployment			
	ADP_{UR}	ESSENZ	ADP_{ER}	SOP_{URR}	ADP_{UR}	ESSENZ	ADP_{ER}	SOP_{URR}
Aluminum	0.00	0.35	0.00	117.90	0.00	0.79	0.01	261.12
Copper	2.41	0.59	0.44	197.98	5.05	1.24	0.93	414.55
Indium	0.01	12.75	63.30	9.88	0.01	29.17	144.79	22.60
Lead	0.01	0.01	0.02	0.48	0.02	0.02	0.03	1.02
Silicon	0.00	0.57	0.00	36.66	0.00	1.26	0.00	80.59
Silver	0.47	0.61	0.45	14.87	1.04	1.35	0.99	32.53
Tin	0.10	1.30	0.10	11.51	0.23	2.89	0.22	25.49
Zinc	0.01	0.05	0.03	1.28	0.02	0.11	0.08	2.7
Gold	4.09	0.10	0.11	19.51	8.57	0.21	0.24	40.88
TOTAL	**7.1**	**16.3**	**64.4**	**410.1**	**14.9**	**370.**	**147.3**	**881.5**
Reduction due to closed-loop recycling [%]	**25.1**	**11.7**	**6.8**	**22.6**	**16.6**	**7.9**	**5.4**	**14.8**

C. APPENDIX: DETAILED RESULTS FOR THE FUTURE ANNUAL END-OF-LIFE PV SYSTEM OUTFLOWS

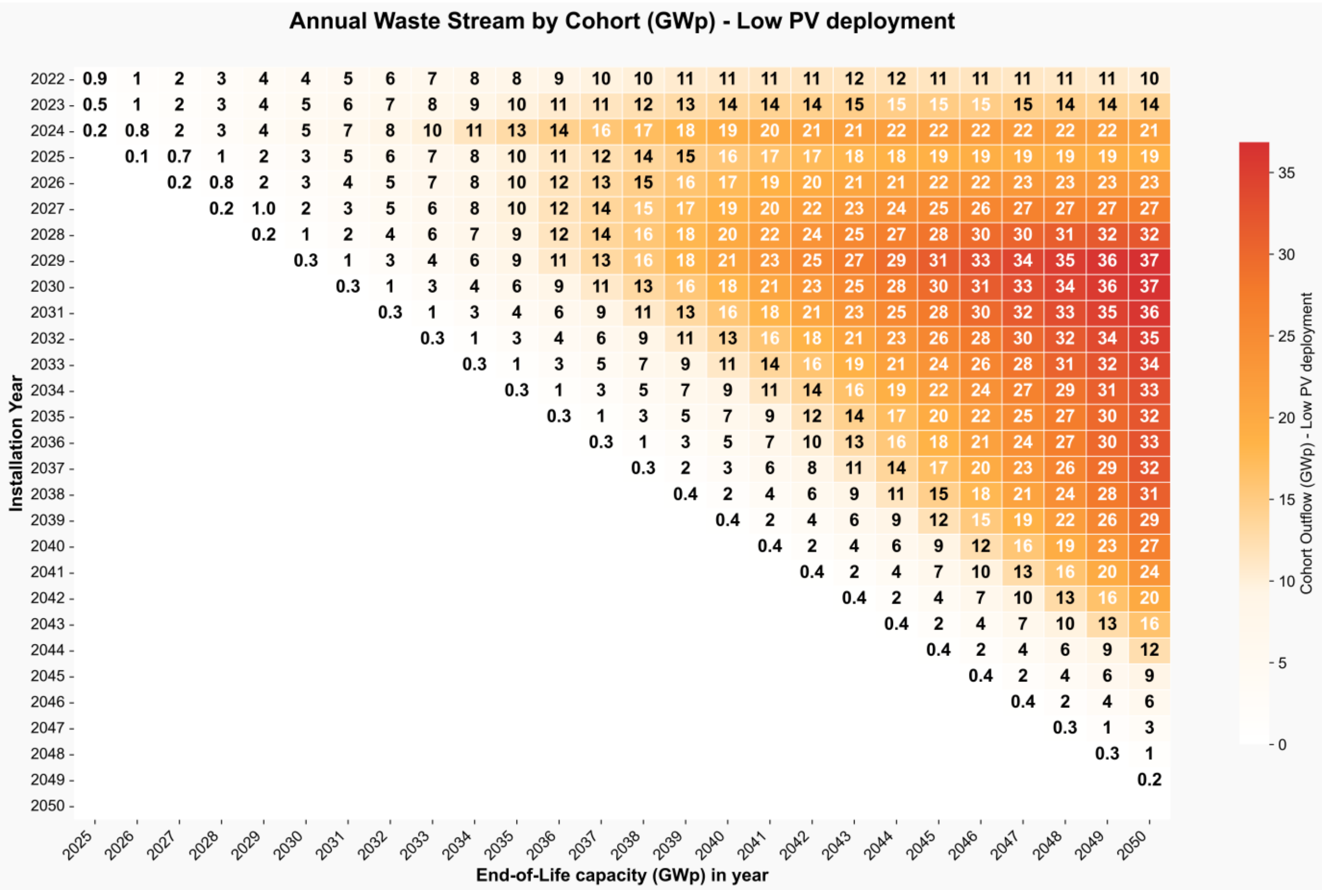

Figure C-1: Cohorts of Annual End-of-Life Outflows in GWp by Installation and Retirement Years-Low Deployment Scenario

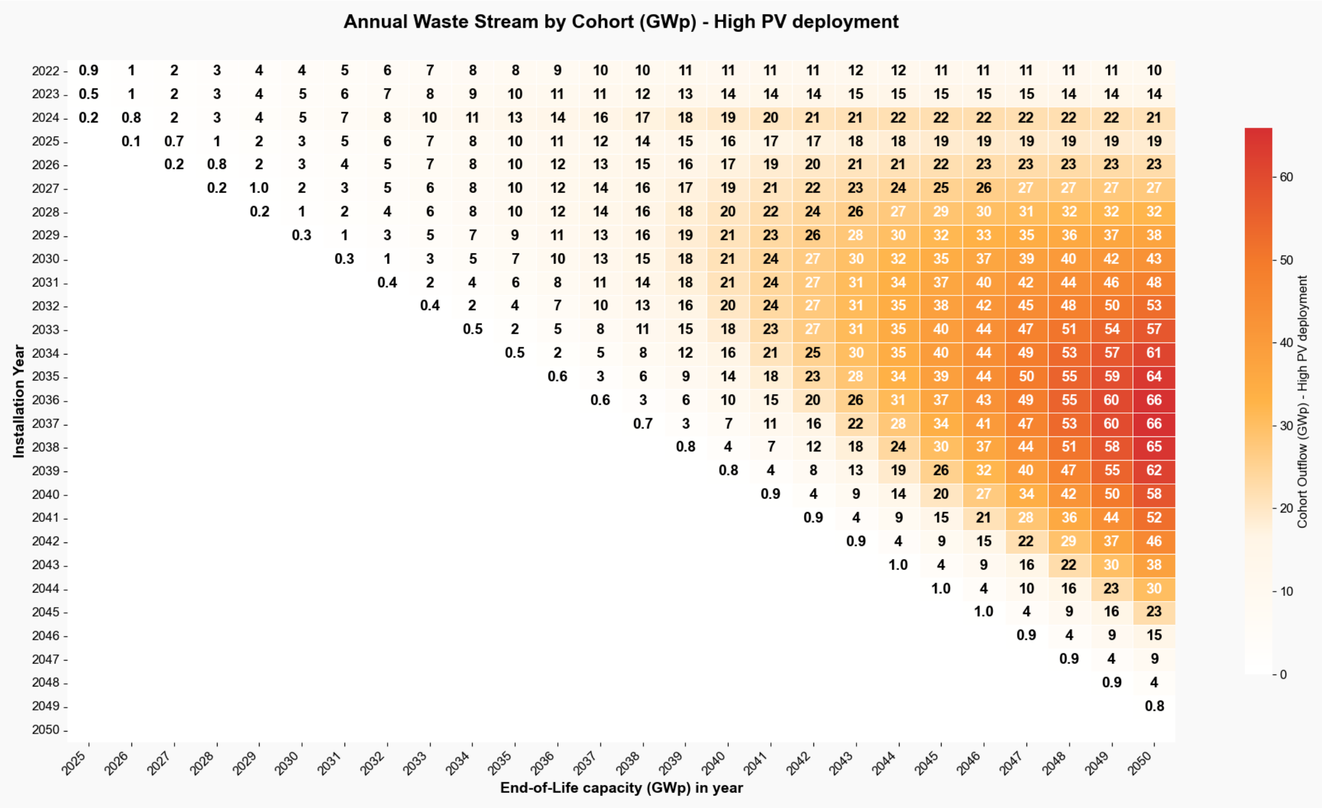

Figure C-2: Cohorts of End-of-Life PV system outflows (GWp) by installation and retirement Years-High Deployment Scenario

D. APPENDIX: ADDITIONAL RESULTS FOR IN-USE STOCK AND ANNUAL MATERIAL FLOWS

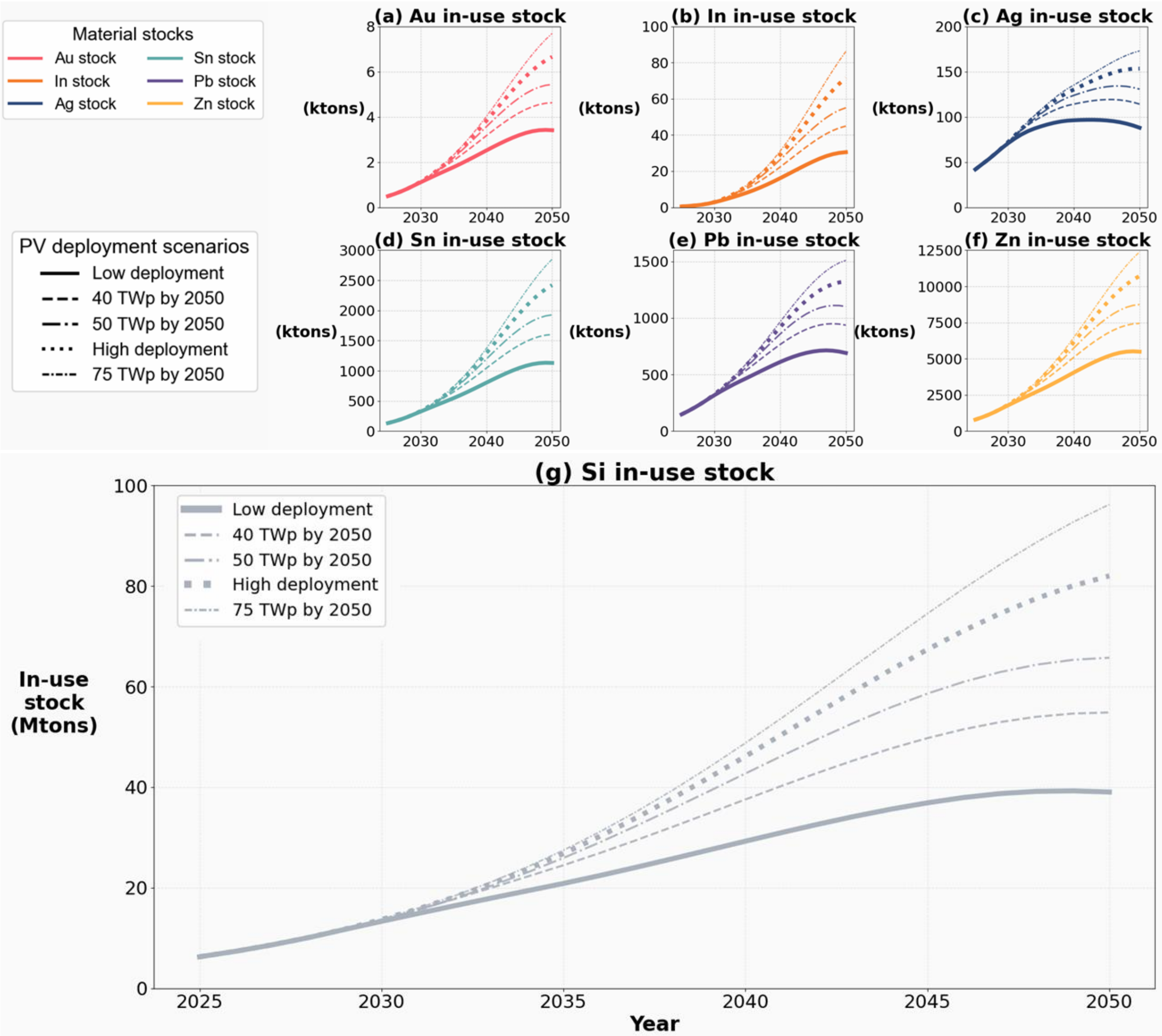

Figure D-1: PV raw materials content in the in-use stock for the five deployment scenarios. (a) gold, (b) indium, (c) silver, (d) tin, (e) lead, (f) zinc, and (g) silicon

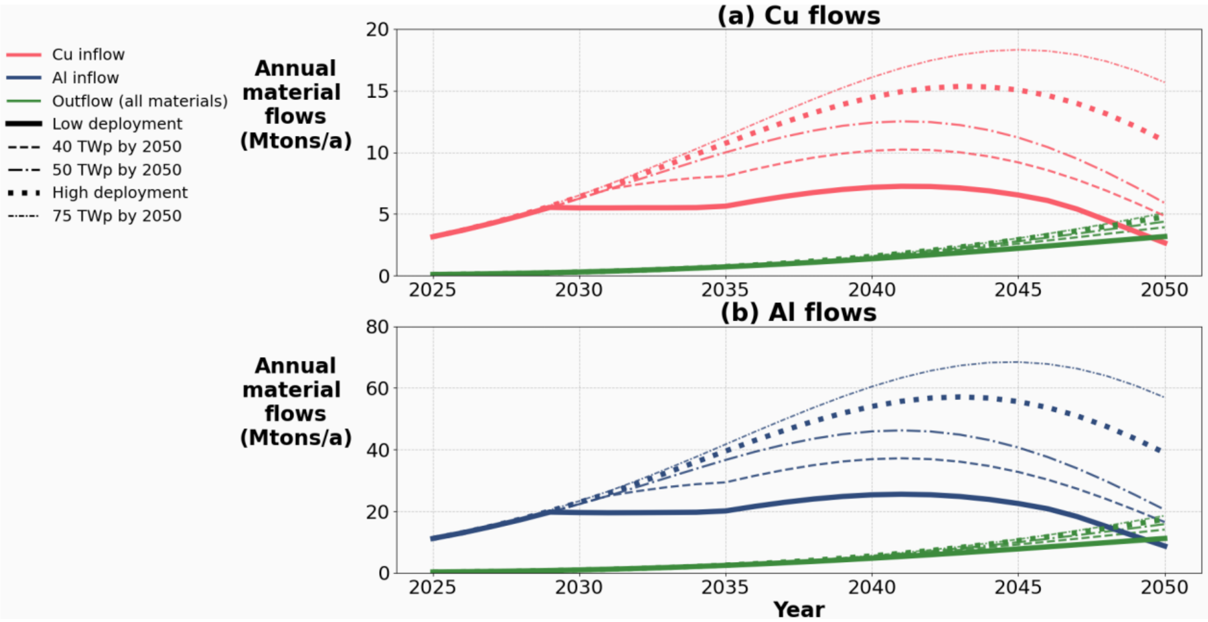

Figure D-2: Forecasted annual inflow demand and secondary supply of PV raw materials for the five deployment scenarios. (a) copper, (b) aluminum

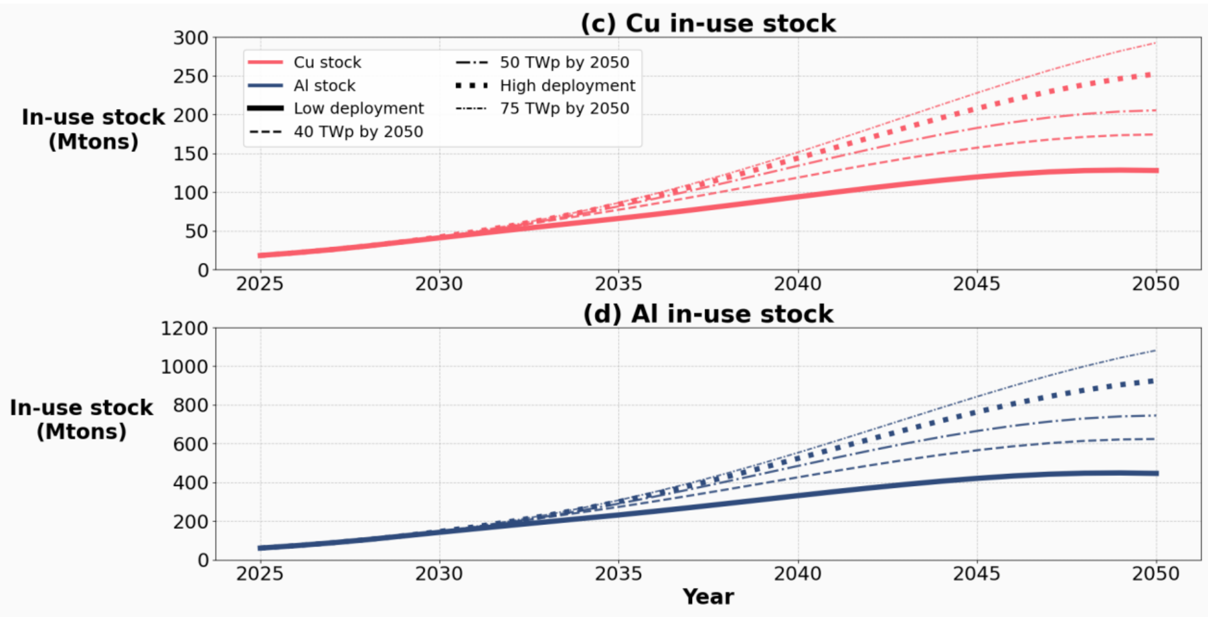

Figure D-3: PV raw materials content in the in-use stock for the five deployment scenarios. (a) copper, (b) aluminum

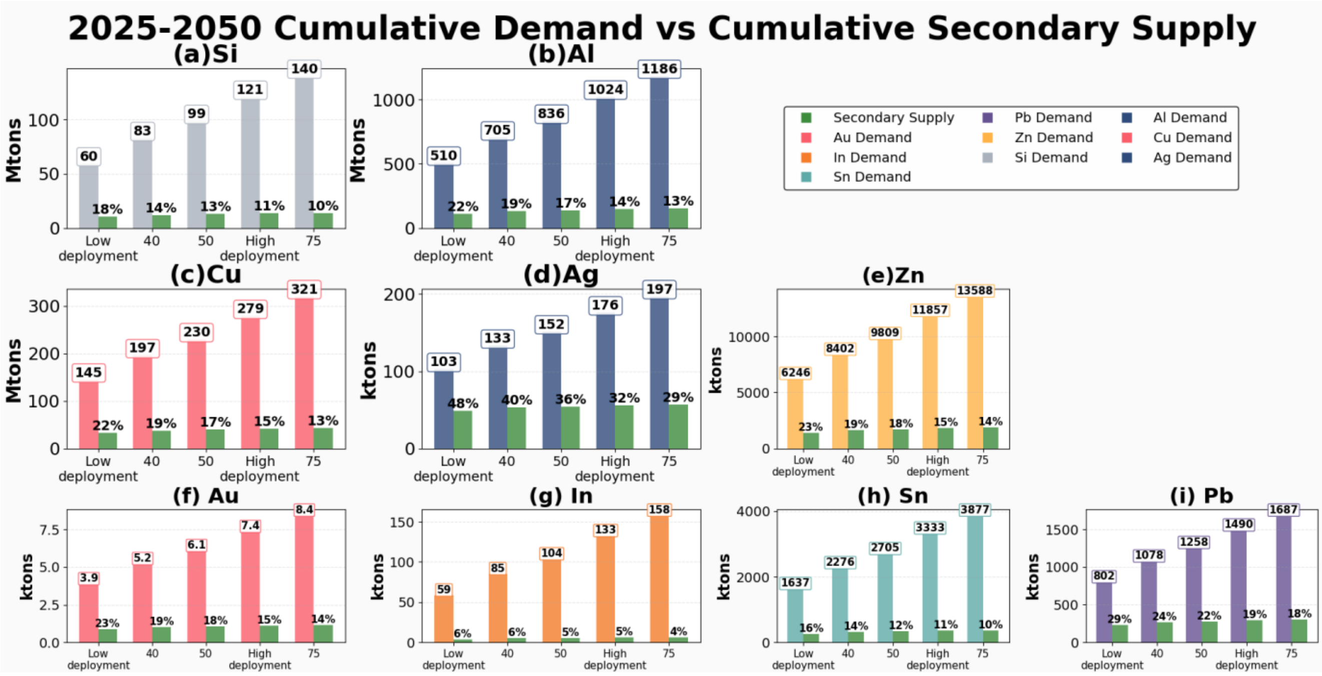

Figure D-4: Cumulative demand (in ktons/Mtons) and cumulative secondary supply (as a % of cumulative demand) of PV raw materials for the five deployment scenarios. (a) silicon, (b) aluminum, (c) copper, (d) silver, (e) zinc, (f) gold, (g) indium, (h) tin, and (i) lead

E. APPENDIX: SENSITIVITY ANALYSIS RESULTS FOR THE CUMULATIVE PV RAW MATERIAL DEMANDS

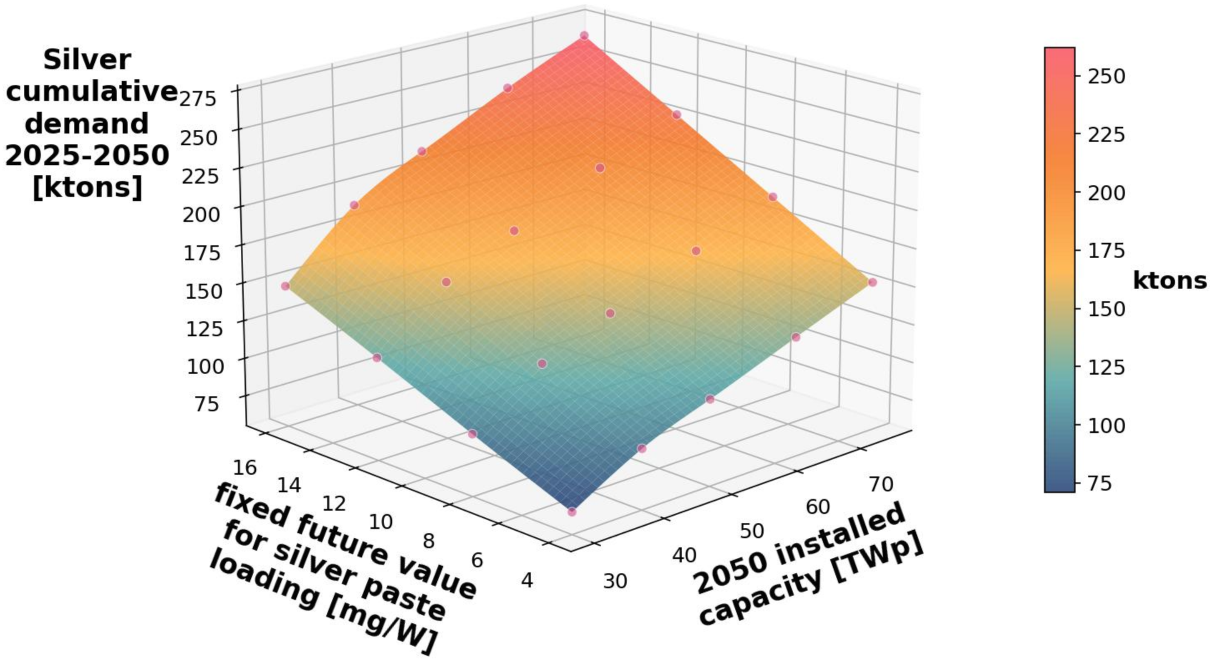

Figure E-1: Cumulative silver demand (2025-2050) as function of silver paste loading and future installed capacity

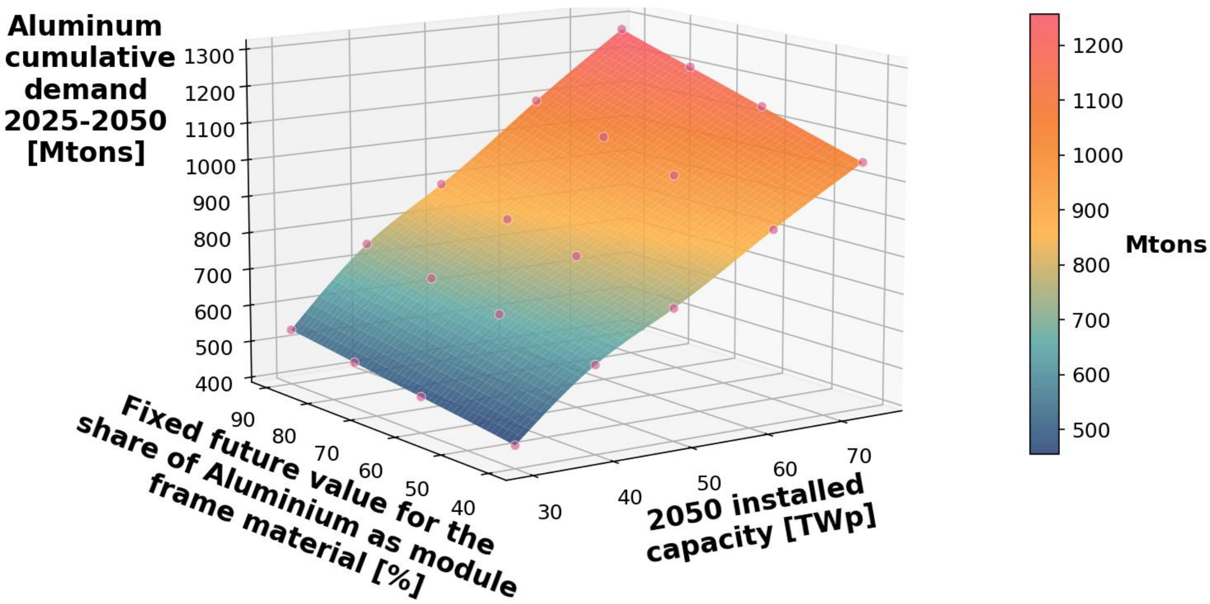

Figure E-2: Cumulative aluminum demand (2025-2050) as function of the market share of aluminum module frames and future installed capacity

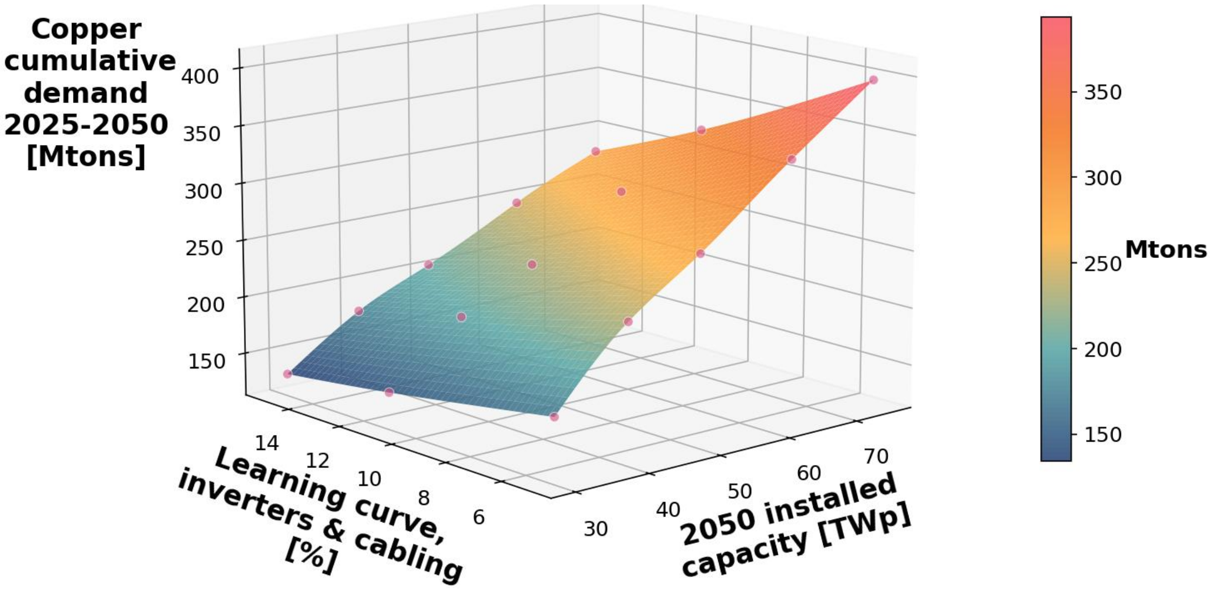

Figure E-3: Cumulative copper demand (2025-2050) as function of the learning curve of inverters and cabling and future installed capacity

Technology Collaboration Programme

by iea